BIOMAT EFFECTS ON WASTEWATER INFILTRATION FROM ONSITE SYSTEM DISPERSAL TRENCHES

by

SHELBY DEE FINCH

(Under the direction of Larry T. West)

ABSTRACT

The objective of this study was to evaluate the reduction in water movement rates associated with biomat formation in common soils in Georgia. Saturated hydraulic conductivity (K_s) was measured on undisturbed cylindrical (7.6/9 cm diameter by 7.6/9 cm length) soil cores collected from the bottom and sidewall of mature dispersal fields and from adjacent un-impacted soil of seven sites in the Georgia Piedmont and Coastal Plain. Four sites had 34 to 93% K_s reduction in samples from dispersal field trenches as compared to natural soil. Lack of K_s reduction was attributed to K_s variability, low K_s, and variability in biomat development because of system design and installation. Model simulations, using Hydrus-2D, indicated that 99.8 % flow through the trench bottom was 99.8% for the Coastal Plain system and 67.8 % for the Georgia Piedmont. Low sidewall biomat hydraulic resistance increased flow through the biomat-affected sidewall soil and decreased ponding.

INDEX WORDS: Organic material, onsite wastewater management system, biomat, saturated hydraulic conductivity

BIOMAT EFFECTS ON WASTEWATER INFILTRATION FROM ONSITE SYSTEM DISPERSAL TRENCHES

by

SHELBY DEE FINCH

B.S.A., The University of Georgia, 2003

A Thesis Submitted to the Graduate Faculty of The University of Georgia in Partial Fulfillment of the Requirements for the Degree

MASTER OF SCIENCE

ATHENS, GEORGIA

2006

BIOMAT EFFECTS ON WASTEWATER INFILTRATION FROM ONSITE SYSTEM

DISPERSAL TRENCHES

by

SHELBY DEE FINCH

Approved:

Major Professor: Larry West

Committee: Miguel Cabrera
David Radcliffe

Electronic Version Approved:

Maureen Grasso
Dean of the Graduate School
The University of Georgia
May 2006

DEDICATION

This thesis is dedicated to God, family, and friends. You were there when I needed support, guidance, and an extra push. Thank you so much.

ACKNOWLEDGEMENTS

Dr. Larry T. West, Dr. Radcliffe, Dr. Cabrera, Vicki Hufstetler, Coby Smith, Charles Moore, Troy Smith, Gus McCormick, Dr. Steve Morris, and the Crop and Soil Science Department. Thank you all very much.

TABLE OF CONTENTS

LIST OF TABLES

Page

LIST OF FIGURES

Page

CHAPTER 1

INTRODUCTION

Onsite wastewater management systems (OWMS) are a cost-effective, environmentally benign method to manage household wastewater if properly installed on suitable soils and properly maintained. Two main reasons for treating wastewater is to protect the environment by preventing pollution and to protect public health by safeguarding water supplies and preventing the spread of water-borne diseases (Gray, 2004; Gerardi and Zimmerman, 2005). In 1990, the U.S. Census Bureau estimated that 24% of the homes in the United States use OWMS to manage household wastewater including about 41% of homes in Georgia (U.S. Census Bureau, 1990a and USEPA, 2002). From 1995 to March 2000, the amount of homes built in Georgia was 16.6% of the total homes built in the United States (U.S. Census Bureau, 2000b). The increase in the number of homes has increased the need for wastewater disposal and the necessity for reevaluating OWMS' long-term wastewater infiltration rates.

One feature that affects hydraulic performance of OWMS is the development of a biomat or clogging mat due to accumulation of organic matter, suspended solids, microorganisms, and fine particles that plug pores at the dispersal trench's soil interface. Biomat development clogs pores, reduces the long-term rate of wastewater infiltration (Laak, 1970), and eventually, may result in hydraulic failure of the system (Beach and McCray, 2003). Beach and McCray (2003) demonstrated by modeling two-dimensional flow in OWMS, with coarse sand-textured and silt-textured soil, that increased biomat development reduced infiltration rates by about 50%. The longevity of an OWMS is closely proportional to the rate of biomat formation and reduction of the long-term acceptance rate (Beach and McCray, 2003; White and West, 2003).

There is a lack of data on biomat saturated hydraulic conductivity (K_s) and thickness needed for model simulations to evaluate the impact of biomat formation on long-term wastewater infiltration rates for soils and conditions in Georgia. Therefore, this study was initiated to evaluate changes in K_s for soils and OWMS in Georgia due to biomat development. The hypothesis is that biomat formation reduces wastewater infiltration rates from OWMS.

Specific objectives are:

1. Evaluate the impact of biomats on infiltration rates from onsite wastewater management systems (OWMS)
2. Evaluate the thickness and porosity of biomats from the bottom and sidewall of the dispersal trench
3. Use data from objectives 1 and 2 to derive biomat K_s
4. Calculate flow from the trench bottom and sidewall of dispersal trenches placed in sand-textured and clay loam-textured soils using two-dimensional models

CHAPTER 2

LITERATURE REVIEW

Onsite Wastewater Management Systems

Onsite wastewater management systems (OWMS) have disposed of household waste for many years because of the close proximity to generated wastes, low costs, and low energy expenditures. Proper wastewater treatment will protect the environment and public health by safeguarding water supplies, preventing pollution of the environment, and preventing the spread of water-borne diseases (Gray, 2004; Gerardi and Zimmerman, 2005). One feature that affects the hydraulic performance of OWMS is the development of a biomat, which is the accumulation of organic matter, suspended solids, microorganisms, and fine particles at or beneath the infiltrative surface.

Typical residential water use is 227 L $person^{-1}$ d^{-1} having total suspended solids (TSS) of about 155 to 300 mg L^{-1}, 5-d biological oxygen demand (BOD) of 155 to 286 mg L^{-1}, and chemical oxygen demand (COD) of 500 to 660 mg L^{-1} (USEPA, 2002). Residential wastewater also has a concentration of total N of 26 to 75 mg L^{-1}, ammonium (NH_4^+) of 4 to 13 mg L^{-1}, nitrites and nitrates (NO_2-N and NO_3-N) of <1 mg L^{-1}, and total phosphorus of 6 to 12 mg L^{-1} (USEPA, 2002). The concentration of total coliform is 10^8 to 10^{10} mg L^{-1}, while fecal coliform concentrations range from 10^6 to 10^8 mg L^{-1} (USEPA, 2002). With all these particles in the wastewater added to the soil on a daily basis, it is important to understand the impact of pore clogging and biomat development on the OWMS' long-term wastewater infiltration.

An OWMS usually consists of a septic tank discharging wastewater effluent to a dispersal field, which treats the effluent by passing it through soil. Studies reported that soil has two functions, renovation and transmission of liquid. These two functions are affected by biomat formation (Gray, 2004; Winneberger, 1984; Van Cuyk, 2001; Laak, 1970). The impact of biomat formation on wastewater infiltration rates can be evaluated by comparing the resistance values of biomat-affected soil to natural soils, as well as by modeling two-dimensional flow simulations with the use of biomat K_s and thickness data.

Septic Tank

Since many state health boards link disease with poorly treated wastewater, the septic tank is crucial to better wastewater management (USEPA, 2002). A septic tank is a watertight buried pretreatment unit for raw sewage and designed to allow the solids to separate by settling, floating, or being digested (Perkins, 1989; Georgia Dep. of Human Resources, 1998). The pretreatment of the raw sewage by the septic tank will prevent the large soil-clogging solids from getting to the dispersal field. The settled solids in the wastewater form sludge while the floating particulate matter forms a layer of scum; both undergo microbial decomposition (Kaplan, 1987). The microbial decomposition reduces the sludge volume by about 40% (Georgia Dep. of Human Resources, 1998). The septic tank is ineffective in removing N. However, anaerobic decomposition converts the organic nitrogen into ammonium (NH_4^+). Because there is a lack of oxygen, the amounts of NO_2^- and NO_3^- concentrations are low in the septic tank (Canter and Knox, 1985). The smaller organic materials in the greenish clear liquid, between the layer of scum and sludge, also undergo some anaerobic decomposition. When displaced by fresh wastewater, the liquid will trickle to the dispersal field (Kaplan, 1987).

Dispersal Field

The dispersal field is a subsurface infiltration system comprised of excavated trenches that are designed to receive a dispersal line, which consists of a perforated pipe of trench length and typically surrounded by gravel (USEPA, 2002; Georgia Dep. of Human Resources, 1998). The surface area of a trench is determined from local regulatory codes that vary across the nation, and are based upon the volume of treated sewage and the soil characteristics in which the dispersal field is located (Perkins, 1989; Georgia Dept. of Human Resources, 1998). Conventionally, the dispersal line is surrounded by washed gravel that provides support for the pipe; however, system designs can vary. Other subsurface infiltration systems would include chamber and expanded polystyrene systems (EPS). The chamber system is a configuration of plastic domes that provides support for the surrounding soil and allows wastewater effluent to filter. The EPS system is also a configuration of perforated pipes but surrounded by polyethylene netting filled with recycled polystyrene (EZflow, 2000).

Soil

After the wastewater effluent infiltrates into the soil, it percolates through the soil. The renovation and transmission of the wastewater by the soil is affected by wastewater components, soil texture, porosity, infiltration rate, and saturated hydraulic conductivity (Tyler et al., 1991).

Renovation

Proper wastewater treatment in the soil will prevent groundwater and surface water contamination by removing NO_3^-, PO_4^{-3}, bacteria, viruses, heavy metals, and other harmful chemicals (i.e. pesticides, acetone) as effluent passes through the soil

(Winneberger, 1984). Under aerobic conditions, nitrification converts ammonium (NH_4^+) into nitrite (NO_2^-) and nitrate (NO_3^-), with NO_3^- being the predominant product (Canter and Knox, 1985; Gray, 2004; Havlin et al., 1999). Nitrogen in the form of NO_3^- is soluble and mobile in the soil because of its anionic form. Soils that are coarse textured (i.e. sand) or that have good structure ensure rapid exchange of gases for nitrification to occur. On the other hand, in more clayey soils or soils with weak structure, incomplete nitrification may occur (Canter and Knox, 1985). In the absence of oxygen, denitrification will reduce NO_3^- to nitrous oxide (N_2O) or nitrogen gas (N_2), which is a biological process performed by facultative heterotrophs (Canter and Knox, 1985).

Humus and clay particles provide a large surface area for ion exchange with ions bonded onto soil particles (Gray, 2004). Another way wastewater chemicals can be renovated by the soil is Fe/Al oxides and clay minerals adsorbing negatively charged ions. Orthophosphate (PO_4^{-3}, HPO_4^{-2}, $H_2PO_4^-$ and H_3PO_4) is the dominant inorganic form of phosphorus in wastewater, and will adsorb to the surfaces of Fe/Al oxides and clay minerals in acidic soils or precipitate as secondary minerals (Canter and Knox, 1985; Havlin, 1999). Bacteria and viruses can also be adsorbed by soils with a neutral or acidic pH, because the negative charge on the bacteria and virus' surface will adsorb to the cation adsorbed to the clay and Fe/Al oxides (Canter and Knox, 1985). Since bacteria are generally the same size as clay particles (1-2 μm), they can be physically strained or filtered by fine soil particles such as clay and silt (Canter and Knox, 1985). In addition, if bacteria were present in large colonies then movement in larger pores would be slower.

By removing bacteria and organic materials, suspended particles accumulate at the infiltrative surface, which clogs soil pores and contributes to the physical straining.

Van Cuyk et al. (2001) applied 5.0 or 8.4 $cm^2\ d^{-1}$ of septic tank effluent (STE) to four lysimeters containing sand. The lysimeters had an aggregate-free (chamber) or aggregate-laden (washed gravel) surface with a 60 or 90 cm soil depth above the water table. After applying STE for one year, a brown to black clogging zone or biomat developed within the upper few cm of the sand. Gradual development of the biomat enhanced the removal of microorganisms, organic constituents, and viruses, but only had a limited removal of nutrients (Van Cuyk et al., 2001). Formation of a biomat enhanced soil, biomat, and wastewater contact before wastewater percolated through the vadose zone. Nitrification and die-off of bacteria tended to occur near the infiltrative surface (upper 30 cm) and decreased with depth (Van Cuyk et al., 2001).

Transmission of liquids

The infiltration rate of wastewater is reduced by soil slaking, dispersion, gravel fines, and biomat formation (organic matter accumulation) at the trench-soil interface. Soil slaking occurs when a soil's cohesive strength is reduced by swelling and entrapped air results in the breakdown of the soil aggregate (Hillel, 2004). Slaking at infiltration surfaces can often form a surface seal, which is a layer of dispersed soil that clogs macropores and will decrease the infiltration rate (Hillel, 2004). High amounts of Na^+ in wastewater can cause dispersion; as a result, infiltration rates are lowered. Many household products contain Na^+ such as bleach, drain opener, and the Na^+ salts added to water softeners that may enhance dispersion and reduce soil K_s (Amoozegar and Niewoehner, 1998).

An OWMS factor that reduces infiltration rates that is not affected by the wastewater components or loading is the medium supporting the dispersal line (i.e.

gravel, expanded polystyrene). Amerson et al. (1991) measured the affects of soil compaction by falling gravel, gravel fines (sandy loam texture), and masking of the infiltrative surface by gravel on wastewater infiltration rates in a sand textured C horizon and silty clay loam Bt horizon. Results indicated when soils were subjected to gravel compaction, contact area reduction, and gravel fines there was a significant effect on the infiltration rate on both soil types. However, gravel fines was the only single factor that had a significant effect on the infiltration rate in the silty clay loam soil. Gravel fines had no effect in the sand textured C horizon (Amerson et al., 1991). It was expected that the greater difference in texture between the soil and gravel fines would result in a greater impact on the infiltrative rate (Amerson et al., 1991).

Biomat formation occurs when microbial activity, bacterial polysaccharides, suspended solids, and organic matter accumulate at the infiltrative surface of the OWMS because of wastewater infiltration (Laak, 1970; Beach and McCray, 2003; Van Cuyk et al., 2001). It has been hypothesized that the accumulated organic matter undergoes humification, gradually filling the soil pores and reducing infiltration rates (Siegrist and Boyle, 1987). The net effect of long-term wastewater infiltration is soil clogging, which forms an inhibiting layer at the infiltrative surface and results in a reduction of the infiltration rate (Jones and Taylor, 1965; Magdoff and Bouma, 1975; Siegrist, 1987; Siegrist and Boyle, 1987; Winneberger, 1984).

As seen in Fig. 2-1, the infiltration rate decreases in three phases with wastewater addition (Thomas et al., 1966; Winneberger, 1984). The first phase is under aerobic conditions with the accumulation of organic matter, iron, phosphate, polysaccharides, and polyuronides occurring within the upper few centimeters of soil (Thomas et al., 1966).

Accumulation of these constituents continues in phase two. However, the environment becomes anaerobic due to wastewater ponding as the soil pores become more completely clogged. Phase three leads to an anaerobic system where clogging has caused infiltration rates to reach minimum values (Fig. 2-1). The optimum design-loading rate through an OWMS would be the soil's K_s (Fig. 2-1). However, soil clogging reduces the hydraulic loading rate of the soil, and the new design-loading rate is the minimum infiltration rate after pores have become clogged (Fig. 2-1).

Few research studies have quantified biomat thickness due to difficulty in measurement (Jones and Taylor, 1965; Laak, 1970; Magdoff and Bouma, 1975; Siegrist, 1987; Thomas, 1966; Winneberger, 1984). Thomas et al. (1966) demonstrated by applying STE to Ottawa sand-filled lysimeters that a mature biomat formed and that 87% of the reduced infiltration rate occurred within the upper 1 cm of the soil. Laak (1970) applied STE to soil columns filled with medium sand, sandy loam, and garden soil, which had developed a clogging zone that was 0.5 cm thick. Siegrist (1987) also reported a biomat thickness of <0.5 cm in silty clay loam textured soil cells applied with STE.

Thicker biomats were reported by Jones and Taylor (1965), Winneberger (1984), and Magdoff and Bouma (1975). Jones and Taylor (1965) applied STE to coarse, medium, and fine sand overlain with gravel. The mature biomat thickness was estimated to be <4 cm from hydraulic head measurements; however, based on visual observations the biomat thickness was suggested to be at the gravel-soil interface. Winneberger (1984) applied STE to Oakley sand filled soil cores, which formed a biomat and reduced the soil's permeability. Winneberger (1984) measured the depth of the biomat as within the upper 2.54 cm of the soil and the soils below that depth remained unaffected.

Magdoff and Bouma (1975) applied STE to sand textured soil overlain with gravel and silt loam soil that was packed in cylindrical columns. The reported biomat thickness was in the upper 3 cm of the sand. These studies (Jones and Taylor, 1965; Laak, 1970; Magdoff and Bouma, 1975; Siegrist, 1987; Thomas, 1966; Winneberger, 1984) suggest a biomat thickness range of <0.5 cm to <4 cm.

In a study using sand-filled lysimeters dosed with STE, soil clogging decreased the rate of infiltration in the area closest to the point of wastewater effluent loading; thereby, increasing the portion of the sand surface being used for infiltration (Van Cuyk et al., 2001). The reduction in infiltration rate was speculated to be from TSS that were clogging the pore openings. Low infiltration rates and soil clogging were correlated to high amounts of wastewater TSS and BOD (Laak, 1970). Because biomat formation is related to TSS and BOD concentrations, pretreatment of wastewater could possibly increase the service time of the system (Laak, 1970).

The service life of an OWMS is related to the hydraulic performance, which is correlated to the clogging zone development and long-term infiltration rate (Beach and McCray, 2003; Van Cuyk et al., 2001). After applying typical household wastewater (1.6 cm d^{-1} and 4.1 cm d^{-1}) for 10 years, Keys et al. (1998) measured the ponding depth and predicted life of mature systems with a biomat in sand-textured soils. At a loading rate of 1.6 cm d^{-1}, the average predicted life of the system was 11 years with an average yearly increase in ponding depth of 27 mm (Keys et al., 1998). At a loading rate of 4.1 cm d^{-1}, the predicted life was 7 years with a ponding depth increase of 44 mm y^{-1}. Because the systems had developed a biomat, long-term infiltration rate and the life of the system was reduced.

Saturated Hydraulic Conductivity and Hydraulic Resistance

Percolation rate (e.g. min cm^{-1}) is the time required for water to seep into saturated soils at a constant rate and can be representative of the soil's adsorptive capabilities during the wettest part of the year (USEPA, 2002). The percolation test is a practical method used to obtain soil absorptive capacity and soil acceptability for septic tank practices and design sizes for dispersal fields (USEPA, 2002; Winneberger, 1984). The infiltrative capacity of the soil typically determines the life of the dispersal field. The saturated hydraulic conductivity can be obtained and correlated to the infiltrative surface infiltration rate (Canter and Knox, 1985).

As discussed earlier, the soil-clogged infiltration rate or K_{eff} will result in a new design-loading rate (Fig. 2-1). Amoozegar and Niewoehner (1998) reported the infiltration rates of sand and clay textured soil by applying car wash wastewater, $CaCl_2$ solution after car wash wastewater, laundry wastewater, and $CaCl_2$ solution after laundry wastewater. On the average, the infiltration rate of the sand-textured soil decreased from 960 cm d^{-1} to 124.8 cm d^{-1}, while the clay textured soil reduced to 0.96 cm d^{-1}. Jones and Taylor (1965) found that the average K_{eff} ranged from 1.83 to 7.32 cm d^{-1} for biomat-affected coarse and fine sand. Furthermore, it was assumed complete clogging of the pores never occurred because the K_s never reached zero. Bouma (1975) conducted a study on 12 subsurface seepage systems and obtained the biomat resistance and the infiltration rate for biomat-affected trench bottom and sidewall soils with different textures. For the sand-textured soil, the K_s was 500 cm d^{-1} that was reduced to 6.6 to 7.5 cm d^{-1} for the trench bottom soil and 1.7 to 9.2 cm d^{-1} for the trench sidewall due to biomat formation. The biomat resistance at the trench bottom was 4.6 to 7.1 d and the biomat resistance at the trench sidewall was 3.2 to 35 d. For the clay soil K_s was 3 cm d^{-1}. The biomat-affected soil of the trench bottom had infiltration rates ranging from 0.17 to 0.75 cm d^{-1}, while infiltration rate of the trench sidewall was 0.17 to 0.62 cm d^{-1}. The biomat resistance at the trench bottom was 28 to 115 d, while the biomat resistance at the trench sidewall was 30 to 115 d (Bouma, 1975).

Magdoff and Bouma (1975) measured the tensions below four sand-textured clogged seepage beds to calculate crust resistance. The systems ranged in age from 1 to 12 yr and had an average crust resistance of 5 d with tensions below the crust ranging from 23 to 27 cm. Magdoff and Bouma (1975) indicated that even though the soil's K_s may be high, increased soil clogging or resistance will result in a reduction of wastewater infiltration rates.

Modeling Two-Dimensional Flow

A software package known as Hydrus-2D can be used to model two-dimensional water flows in variably saturated media by specifying the soil's hydraulic parameters (e.g. K_s for specified textures, etc.) (Rassam et al., 2003). Because there is no analytical solution to the Richard's (1931) equation, using numerical models to calculate flow is a very useful tool.

Beach and McCray (2003) modeled two-dimensional flow in OWMS for a sand and silt soil and achieved unsaturated conditions by using wastewater loading less than the soil's K_s. The natural sand and silt soil had a K_s of 2000 and 40 cm d^{-1}, respectively. The coarse sand and silt textures with shallow ponding (4 to 10 cm) had bottom and sidewall K_{eff} values of 6.0 cm d^{-1} and 7.44 cm d^{-1} respectively, while the K_{eff} for the trench bottom and sidewall was 1.5 cm d^{-1} and 2.16 cm d^{-1} for coarse sand and silt textures with deep ponding (20 to 23 cm). The results from the models indicated that the hydraulic properties of the clogging zone and subsoil contributed to the flow rate and water content distributions within the OWMS (Beach and McCray, 2003).

The average water velocity and residence time for a shallow ponded trench bottom with sand textured soil were 29 cm d^{-1} and 2.1 d, while for the deep-ponded system were 25 cm d^{-1} and 2.4 d. The increased hydraulic resistance in the sand systems resulted in decreased water content throughout the system, which increased the wastewater treatment area. The water velocity and residence time were 22 cm d^{-1} and 2.7 d for the silt trench bottom with shallow ponding and 15 cm d^{-1} and 4.0 d for the deep ponding trench bottom. Increased hydraulic resistance for both sand and silt systems increased sidewall flow (Beach and McCray, 2003). Beach and McCray (2003) stated that the silt system had substantially greater residence times than the sand system because of lower overall unsaturated hydraulic conductivity. Because hydraulic residence times are generally correlated to purification processes, the increase from the degree of clogging can be seen as potential enhancement in wastewater treatment.

Radcliffe et al. (2005) modeled flow through the bottom of a trench consisting of a BC and Bt1 horizon in a Cecil soil. The biomat thickness used was 2 cm with K_s of 0.05 cm d^{-1}. The BC horizon K_s was 0.84 cm d^{-1} and the Bt1 horizon K_s was 257.5 cm d^{-1}. Five models were tested per horizon to compare wastewater infiltration rates of an open trench to trenches with gravel masking, embedded gravel, and sidewall flow for the open trench and embedded gravel. There was a negligible effect from gravel masking in the BC horizon, because there was a large gradient at the soil surface next to the gravel particles that pulled the water laterally beneath the gravel. The embedded gravel had a greater effect in reducing infiltration rates (ratio of open trench to gravel of 1.5). When sidewall was included in the open trench and embedded gravel system, the total infiltration rates increased for each system. The open trench infiltration rate increased from 0.31 to 0.43 cm d^{-1} and was 1.33 times greater than the embedded gravel system, while the embedded gravel system's infiltration rate increased from 0.21 to 0.32 cm d^{-1}.

The infiltration rates were higher in the Bt1 horizon than the BC horizon. The open system infiltration rate was 1.34 times greater than the gravel-masked system and 1.93 times greater than the embedded gravel system. When sidewall flow was included, the infiltration rate in the open system increased from 0.75 to 1.04 cm d^{-1} and was 1.7 times greater than the embedded gravel system. The embedded gravel system's infiltration rate increased from 0.39 to 0.61 cm d^{-1}. Sidewall flow allowed more infiltration in both horizons and reduced the affect of the embedded gravel. Radcliffe et al. (2005) results indicated that there was a greater impact on infiltration rates when there is a large difference between the biomat K_s and the natural soil K_s.

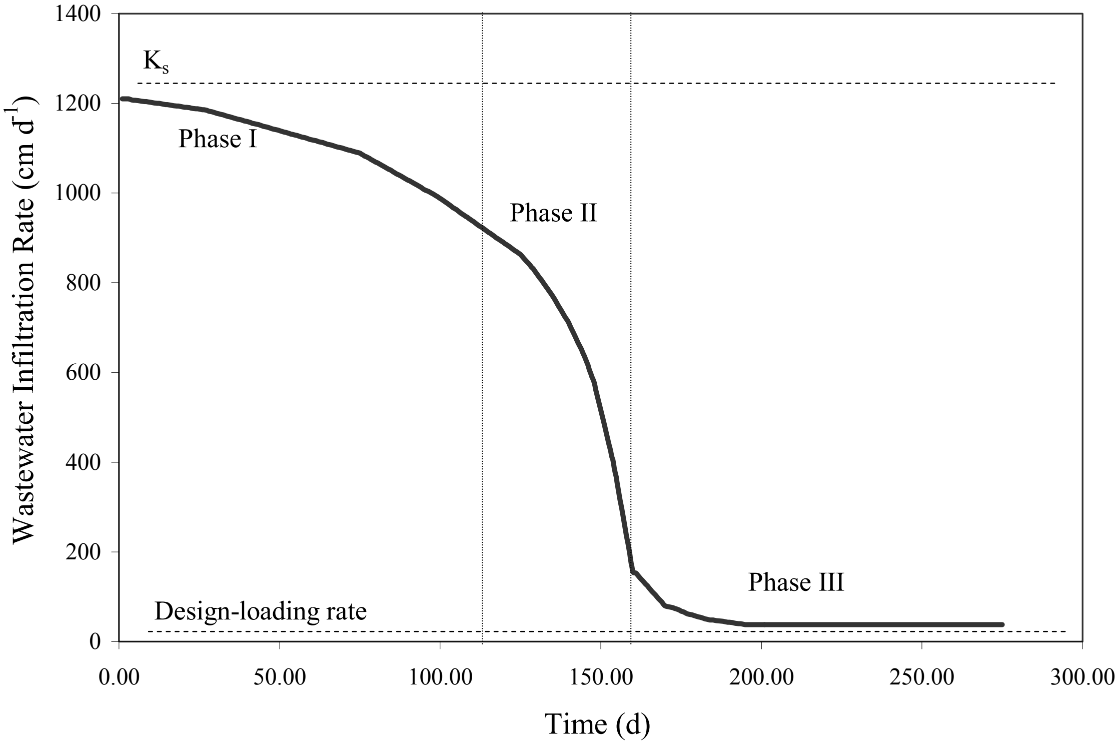

Figure 2-1. Infiltration rate reduction with time under wastewater application: Adapted from Thomas et al., 1966.

References

Amerson, R.S., E.J. Tyler, and J.C. Converse. 1991. Infiltration as affected by compaction, fines, and contact area of gravel. Conf. Natl. Symp. Individual and Small Community Sewage Systems, 6th, Chicago, IL, USA. 16-17 Dec. 1991. ASAE Publ. 10-91:243-247. St. Joseph, MI.

Amoozegar, A. and C.P. Niewoehner. 1998. Soil hydraulic properties affected by various components of domestic wastewater. On-site wastewater treatment. Proc. Natl. Symp. Individual and Small Community Sewage Systems, 8th. ASAE Publ. 3-98:155-166. St. Joseph, MI.

Bouma, J. 1975. Unsaturated flow during soil treatment of septic tank effluent. J. Environ. Eng. Div. Am. Soc. Civ. Eng. 101: 967-983.

Beach, D.N.H., and J.E. McCray. 2003. Numerical modeling of unsaturated flow in wastewater soil absorption systems. Ground Water Monit. Remediation 23:64-72.

Canter, L.W. and R.C. Knox. 1985. Septic tank system effects on ground water quality. Lewis publishers, Inc. Chelsea, MI.

EZflow, 2000. [Online]. Features and benefits. Available at http://www.ezflowlp.com/frames/frproducts.html (Verified 13 Dec. 2005).

Georgia Dep. of Human Resources. 1998. Manual for on-site sewage management systems. Georgia Dep. of Human Resources, Atlanta, GA.

Gray, N.F. 2004. Biology of wastewater treatment. 2nd ed. Imperial College Press, London.

Gerardi, M.H. and M.C. Zimmerman. 2005. Wastewater pathogens. Wiley-Interscience, Hoboken, N.J.

Havlin, J.L., J.D. Beaton, S.L. Tisdale, and W.L. Nelson. 1999. Soil fertility and fertilizers. 6th ed. Prentice Hall, Inc. Upper Saddle River, NJ.

Hillel, D. 2004. Introduction to environmental soil physics. Elsevier Science, USA.

Jones, J.H. and G.S. Taylor. 1965. Septic tank effluent percolation through sands under laboratory conditions. Soil Sci. The Williams and Wilkins Co., USA.

Kaplan, O.B. 1987. Septic systems handbook. Lewis, Chelsea, MI.

Keys, J.R., E.J. Tyler, and J.C. Converse. 1998. Predicting life for wastewater absorption systems. p. 167-176. *In* Proc. of the Eighth Natl. Symp. on Individual and Small Community Sewage Systems, 8th, Orlando, FL, USA. 8-10 Mar. 1998. ASAE Publ. 10-91:192-200. St. Joseph, MI.

Laak, R. 1970. Influence of domestic wastewater pretreatment on soil clogging. J. Water Pollut. Control Fed. Part I. 42:1495-1500.

Magdoff, F. R. and J. Bouma. 1975. The development of soil clogging in sands leached with septic tank effluent. p. 37-47 *In* Proc. of the Natl. Home Sewage Disposal Symp. ASAE Publ. Chicago, USA. 9-10 Dec. 1974. St. Joseph, MI.

Perkins, R.J. 1989.Onsite wastewater disposal. Lewis, Chelsea, MI.

Radcliffe, D.E., L.T. West, and J. Singer. 2005. Gravel effect on wastewater infiltration from septic system trenches. Soil Sci. Soc. Am. J. 69:1217-1224. Madison, WI.

Rassam, D., J. Šimůnek, and M.Th. van Genuchten. 2003. Modeling variably saturated flow with hyrdrus-2d. ND Consult. Brisbane, Australia.

Siegrist, R.L. 1987. Soil clogging during subsurface wastewater infiltration as affected by effluent composition and loading rate. J. Environ. Qual. 16:181-187.

Siegrist, R.L. and W.C. Boyle. 1987. Wastewater-induced soil clogging development. J. Environ. Eng. 113:550-566.

Thomas, R.E., W.A. Schwartz, and T.W. Bendixen. 1966. Soil chemical changes and infiltration rate reduction under sewage spreading. Soil Sci. Soc. Am. Proc., 30:641-646.

Tyler, E.J., E.M. Drozd, and J.O. Peterson. 1991. Estimating wastewater loading rates using soil morphological descriptions. Conf. Natl. Symp. Individual and Small Community Sewage Systems, 6th, Chicago, IL, USA. 16-17 Dec. 1991. ASAE Publ. 10-91:192-200. St. Joseph, MI.

U.S. Census Bureau. 1990a. Housing Characteristics. [Online]. Available at http://factfinder.census.gov/servlet/QTTable?_bm=y&-state=qt&-context=qt&-qr_name=DEC_1990_STF3_DP5&-ds_name=DEC_1990_STF3_&-CONTEXT=qt&-tree_id=100&-all_geo_types=N&-redoLog=true&-geo_id=01000US&-geo_id=04000US13&-search_results=01000US&-format=&-_lang=en (posted 1 April 1990; verified 11 Dec. 2005).

U.S. Census Bureau. 2000b. General Housing Characteristics. [Online]. Available at http://factfinder.census.gov/servlet/QTTable?_bm=y&-context=qt&-qr_name=DEC_2000_SF1_U_QTH1&-ds_name=DEC_2000_SF1_U&-CONTEXT=qt&-tree_id=4001&-all_geo_types=N&-redoLog=true&-_caller=geoselect&-geo_id=01000US&-geo_id=04000US13&-search_results=01000US&-format=&-_lang=en (posted 1 April 2000; verified 12 Dec. 2005).

USEPA. 2002. On-site wastewater treatment systems manual. EPA/625/R-00/008 Office of Water. Office of Research and Development. (Available on-line http://www.epa.gov/ORD/NRMRL/Pubs/625R00008/625R00008.pdf.) (Verified 13 Aug. 2002.)

Van Cuyk, S., R. Siegrist, A. Logan, S. Masson, E. Fischer, and L. Figueroa. 2001. Hydraulic and purification behaviors and their interactions during wastewater treatment in soil infiltration systems. Wat. Res. 35:953-964.

White, K.D. and L.T. West. 2003. In-ground dispersal of wastewater effluent: The science of getting water into the ground. Small Flows Quarterly. 4 vol. no. 2

Winneberger, J.H.T. 1984. Septic-tank systems: A consultant's toolkit. Butterworth, Stoneham, MA.

CHAPTER 3

BIOMAT EFFECTS ON WASTEWATER INFILTRATION FROM ONSITE SYSTEM DISPERSAL TRENCHES

Introduction

Onsite wastewater management systems (OWMS) are a cost-effective, environmentally benign method to manage household wastewater if properly installed on suitable soils and properly maintained. Two main reasons for treating wastewater is to protect the environment by preventing pollution and to protect public health by safeguarding water supplies and preventing the spread of water-borne diseases (Gray, 2004; Gerardi and Zimmerman, 2005). The U.S. Census Bureau estimated that 24% of the homes in the United States use OWMS to manage household wastewater including about 41% of homes in Georgia (U.S. Census Bureau, 1990a and USEPA, 2002).

One feature that affects hydraulic performance of OWMS is the development of a biomat or clogging mat due to accumulation of organic matter, suspended solids, microorganisms, and fine particles that plug pores at the dispersal trench's soil interface. Biomat development clogs pores, reduces the long-term rate of wastewater infiltration (Laak, 1970), and eventually, may result in hydraulic failure of the system (Beach and McCray, 2003). Studies have reported the natural soil K_s being reduced 99.5% by biomat formation (Jones and Taylor, 1965; Siegrist, 1987). The longevity of an OWMS is closely proportional to the rate of biomat formation and reduction of the long-term acceptance rate (Beach and McCray, 2003; White and West, 2003).

Limited research studies have quantified biomat thickness due to difficulty in measurement (Jones and Taylor, 1965; Laak, 1970; Magdoff and Bouma, 1975; Siegrist, 1987; Thomas et al., 1966; Winneberger, 1984). Thomas et al. (1966) demonstrated by applying STE to Ottawa sand filled lysimeters with a mature biomat that infiltration rates reduced 87% and occurred within the upper 1 cm of the soil. Laak (1970) applied STE to soil columns filled with medium sand, sandy loam, and garden soil, which had developed a clogging zone that was 0.5 cm thick. Siegrist (1987) also reported a biomat thickness of <0.5 cm in silty clay loam textured soil cells applied with STE. Thicker biomats were reported by Jones and Taylor (1965), Winneberger (1984), and Magdoff and Bouma (1975). Jones and Taylor (1965) estimated the biomat thickness to be <4 cm from hydraulic head measurements in applied STE to coarse and fine sand overlain with gravel. Based on visual observations the biomat thickness was suggested to be at the gravel-soil interface. Winneberger (1984) applied STE to Oakley sand filled soil cores and measured the depth of the biomat within the upper 2.54 cm of the soil and the soils below that depth remained unaffected. Magdoff and Bouma (1975) applied STE to sand textured soil overlain with gravel and silt loam soil that was packed in cylindrical columns. The reported biomat thickness was in the upper 3 cm of the sand. These studies (Jones and Taylor, 1965; Laak, 1970; Magdoff and Bouma, 1975; Siegrist, 1987; Thomas, 1966; Winneberger, 1984) result in a biomat thickness range of <0.5 cm to <4 cm.

Siegrist (1987) measured in-situ the hydraulic conductivity properties of a dispersal field located in silty clay loam textured soil with percolation rates ranging from 9 to 16 min cm^{-1}. The saturated hydraulic conductivity of the natural soil was 241 cm d^{-1} and dropped to <1.3 cm d^{-1} (99.5%) due to soil clogging. Jones and Taylor (1965) measured the steady hydraulic conductivity rate of sand (coarse and fine) packed columns, overlain with gravel, under continuous percolation for twenty weeks. The sand textured soil K_s ranged from 610 to 1951 cm d^{-1} and reduced to 1.83 to 7.32 cm d^{-1} after biomat formation or 0.30 to 0.34% of the natural K_s. These studies reported K_{eff} values for the biomat-affected soil, but the K_s biomat was not reported due to difficulty in measuring biomat length.

A few other studies (Bouma, 1975; Keys et al., 1998), however, have reported the biomat K_s. Bouma (1975) conducted a study on 12 subsurface seepage systems and obtained the biomat resistance and the infiltration rate for biomat-affected trench bottom and sidewall soils with different textures. For this study, the coarse sand and clay soil will be discussed. The hydraulic resistance of the trench bottom biomat ranged from 4.6 to 7.1 d in the coarse sand and 28 to 115 d in the clay. The biomat K_s of the bottom biomat ranged from 5.8 to 7.5 cm d^{-1} in the coarse sand and 0.17 to 0.75 cm d^{-1} in the clay soil. For the trench sidewall biomat, the hydraulic resistance of the coarse sand was 3.2 to 35 d and 30 to 115 d for the clay soil. The biomat K_s was 1.7 to 9.2 cm d^{-1} in the coarse sand and 0.17 to 0.62 cm d^{-1} for the clay. Keys et al. (1998) had reported biomat K_s values ranging from 0.02 cm d^{-1} for the bottom and sidewall areas to 2.41 cm d^{-1} for the unaffected upper sidewall. The biomat K_s values calculated in this study were within the K_s range reported by Keys et al. (1998).

There is a lack of data on biomat saturated hydraulic conductivity (K_s) and thickness needed for model simulations to evaluate the impact of biomat formation on long-term wastewater infiltration rates for soils and conditions in Georgia. Therefore, this study was initiated to evaluate changes in K_s for soils and OWMS in Georgia due to biomat development. The hypothesis is that biomat formation reduces wastewater infiltration rates from OWMS.

Specific objectives are:

1. Evaluate the impact of biomats on infiltration rates from onsite wastewater management systems (OWMS)
2. Evaluate the thickness and porosity of biomats from the bottom and sidewall of the dispersal trench
3. Use data from objectives 1 and 2 to derive biomat K_s

Theory

The K_s is the proportionality constant for water flux under saturated conditions and is affected by texture, structure, porosity, pore distribution, compaction, soil dispersion, organic matter, and microbial activity. Furthermore, each soil layer provides an extent of hydraulic resistance to effluent flow (White and West, 2003). Similar to an electric circuit, hydraulic resistance in series is additive.

Under saturated conditions, the Henri Darcy's equation (Eq. [1]) can be used to solve for K_s (Eq. [2]) where (Hillel, 1998):

$$Q = -K_s \times A \times \frac{\Delta H}{L} \qquad [1]$$

$$K_s = -\frac{Q \times L}{A \times \Delta H} \qquad [2]$$

Q=volumetric flow rate (cm^3 d^{-1})

K_s=saturated hydraulic conductivity or proportionality constant (cm d^{-1})

L=length of soil (cm)

A=cross-sectional area of soil (cm^2)

ΔH=hydraulic head (cm)

Using Darcy's Law, hydraulic resistance (R) can be derived by solving for hydraulic flux (Eq. [3]) and ΔH (Eq. [4]). Because current is analogous to hydraulic flux (J_w) in Eq. [3] and voltage is analogous ΔH (Eq. [3]), the hydraulic resistance (R) can be derived using Eq. [5].

$$J_w = \frac{Q}{A} = -K_s \times \left(\frac{\Delta H}{L} \right) \qquad [3]$$

$$\Delta H = \frac{-J_w \times L}{K_s} \qquad [4]$$

The soil's resistance can also be calculated by using the soil's length and K_s (Eq. [5]).

$$R = \frac{-\Delta H}{J_w} = \frac{L}{K_s} \qquad [5]$$

The effective hydraulic resistance is the sum of the resistance of the soil layers (Eq. [6]). The effective saturated hydraulic conductivity (K_{eff}) is calculated by solving Eq. [7].

$$R_{eff} = \sum_{z=1}^{N} R_z = \sum_{z=1}^{N} \frac{L_z}{K_z} = \frac{\sum_{z=1}^{N} L_z}{K_{eff}} \qquad [6]$$

$$K_{eff} = \frac{\sum_{z=1}^{N} L_z}{\sum_{z=1}^{N} \frac{L_z}{K_z}} \qquad [7]$$

By using the K_{eff} equation for the biomat-affected soil (Eq. [8]), the K_s of the biomat (K_B) can be calculated using Eq. [9] (White, 2002; White and West, 2003).

$$K_{eff} = \frac{L_B + L_N}{\frac{L_B}{K_B} + \frac{L_N}{K_N}} \qquad [8]$$

$$K_B = \frac{L_B}{\left[\frac{L_B + L_N}{K_{eff}} - \frac{L_N}{K_N} \right]} \qquad [9]$$

K_{eff}=K_s measured on core samples

L_B=thickness of the biomat from thin-section polished block samples

K_B=K_s of biomat

L_S=thickness of soil in core below biomat

K_N=K_s of natural soil and mean measurements taken from natural soil

Materials and Methods

Field Methods

Seven OWMS sites were selected in the GA Piedmont (6) and Coastal Plain (1) for the study. Site selection was based on availability and ease of dispersal field access. The age of the OWMS ranged from 7 to 43 yr. All of the dispersal fields were gravity fed; four were gravel systems, two were chamber systems, and one was an expanded polystyrene system (EPS) (Table 3-1). Owners of each OWMS site provided the details of dispersal field design and age, while approximate loading rates were evaluated from the number of household occupants (Table 3-1).

Sampling consisted of collecting relatively undisturbed soil cores using galvanized steel cylinders (7.6 or 9 cm diameter by 7.6 or 9 cm length) from mature OWMS dispersal field sites. For each location, two or three different sites were excavated and triplicate core samples of both natural and biomat-affected soils (trench bottom and sidewall) were collected from each site (Fig. 3-1). Core samples with both vertical and horizontal orientation were collected from adjacent natural soils at depths corresponding to the dispersal field samples. The cores were collected in such a way that included gravel (for systems for aggregate), biomat, and associated soil.

Soil descriptions and site characteristics were collected at each site and are given in Appendix A. Bulk samples of each horizon at each site were collected and analyzed for particle size distribution (Kilmer and Alexander, 1949) and pH (McLean, 1982) (Appendix B). Undisturbed clods were taken from the trench bottom and sidewall for polished block and thin section preparation.

Saturated Hydraulic Conductivity

To avoid dispersion, the soil cores were saturated with 0.1 M $CaCl_2$ with 1 g additions of Thymol to reduce bacterial growth. Saturated hydraulic conductivity (K_s) was measured using the constant head method with a 0.1 M $CaCl_2$ solution (Klute and Dirksen, 1986; Burke et al. 1986b). The K_s measurement for the biomat-affected cores was an effective saturated hydraulic conductivity (K_{eff}) because the samples evaluated included both trench biomat and natural soil layers (White and West, 2003). The K_{eff} for the biomat-affected samples (trench bottom and sidewall) were compared to the natural soil samples to evaluate if there was reduction in OWMS infiltration rates with biomat formation.

Measurement of Biomat Thickness

After K_{eff} was measured, selected core samples from Sites A, B, and C were treated with glutaric dialdehyde to fix the organic matter in the biomat, dried by acetone replacement, and impregnated with polyester resin containing a fluorescent additive (Uvitex OB). The samples from the other sites were slowly air-dried and impregnated with an epoxy resin (Scotchcast 3M) that also contained Uvitex OB. With additions of fluochromes (fluorescent dyes), pores were made more visible, in the polished blocks or thin-sections, by fluorescence microscopy (Stoops, 2003).

After impregnation was complete, thin-sections and polished blocks were prepared by standard techniques and were used for descriptions of the soil and biomat fabric (Murphy, 1986). Thin-sections and polished blocks were photographed under ultraviolet light to evaluate the amount and size distribution of pores with equivalent circular diameter, > 0.05 mm. The pore distribution with depth was used to evaluate the biomat thickness by taking images at 4-mm increments in three vertical transects within the polished blocks. Subsequently, the images were electronically divided into 1-mm sections to provide greater resolution for thickness evaluation. Images were processed using a public domain image-processing program, Image J, which was created by Wayne Rasband at the National Institute of Mental Health in Bethesda, Maryland (Collins, 2005). The mean porosity for the three transects was graphed at each depth. The depth at which porosity increased to that of the natural soil porosity was considered the lower boundary of the biomat (Fig. 3-2).

Soil-Moisture Characteristic Curve

The soil's water content at different pressures was measured by using Tempe cells and carefully controlled pressure at the top of the cells (Dane and Hopmans, 2002). The Tempe cells were weighed at each pressure step (15 to 765 cm of water).

Gravimetric water content (w) was calculated using Eq. [10] where WET_{Soil} was the wet soil weight and the OD_{Soil} was the oven-dried soil weight. Bulk density (ρ_b) was measured using the excavation and core method (Blake and Hartge, 1986), and then calculated using Eq. [11] where V_{Soil} was the volume of the soil (Appendix C). The volumetric water content (θ) was calculated using Eq. [12] where ρ_l is the density of water (Burke et. al, 1986a). Saturated water content (θ_s) was calculated using Eq. [13], where p_s is 2.65 g cm^{-3}.

$$w = \frac{WET_{Soil} - OD_{Soil}}{OD_{Soil}} \qquad [10]$$

$$\rho_b = \frac{OD_{Soil}}{V_{Soil}} \qquad [11]$$

$$\theta_v = \frac{\rho_b \times w}{\rho_l} \qquad [12]$$

$$\theta_s = 1 - \frac{\rho_b}{\rho_s} \qquad [13]$$

Using the saturated water content (θ_s) and measured data (ρ_b and θ_v), van Genuchten's parameters (n, α, θ_r) were predicted using a nonlinear least squares method (Minerr) in MathCAD to provide the best fit. The van Genuchten model can be seen in Eq. [14] where, θ_v is the volumetric water content at different pressures, θ_r is the residual water content, θ_s is the saturated water content, and α, m ($1-n^{-1}$), and n are fitting parameters.

$$\theta_v = \theta_r + \frac{(\theta_s - \theta_r)}{\left[1 + (\alpha h)^n\right]^m} \qquad [14]$$

The van Genuchten parameters for the natural soil and biomat-affected soil were compared to evaluate the effect of biomat formation.

Statistical Analysis

Statistical analysis software (SAS) was used to analyze the K_{eff} values, bulk density, and van Genuchten's parameters by testing for normality with Proc Univariate (α=0.10). Logarithmic transformations were applied to the K_s values and all of van Genuchten's parameters, except n, to obtain normally distributed data before testing the means. The bulk density values were normally distributed. The difference between the biomat-affected and natural soil K_s means were compared using Proc Glm (α=0.10) with Tukey's least significant differences.

Results and Discussion

Natural Soil K_s

There was no significant difference between the natural vertical and horizontal K_s means within Sites B, C, D, E, and F (Table 3-2). Therefore, natural vertical and horizontal K_s values were averaged as one natural K_s value for each site (Table 3-3). The detection limit for K_s measurements was 0.01 cm d^{-1}. The K_s range was from < 0.01 cm d^{-1} (Site C) to 41 cm d^{-1} (Site G) (Table 3-3). The trench bottoms of Site A, C, D, E, and F were installed in sandy clay loam to clay textured soil horizons and all except Site A had low K_s values. At Site B and G, the soil textures ranged from loam to sand.

Assuming that K_s is equivalent to 7% the inverse of the percolation rate, the K_s from each site can be converted to a percolation rate to evaluate its suitability for an onsite system dispersal field in Georgia (Radcliffe and West, 2000). The acceptable percolation rates must be 35.4 min cm^{-1} or K_s greater than 2.8 cm d^{-1} (Georgia Dept. Human Resources, 1998). The only sites that would have acceptable rates would be Site A and G (Table 3-3). Although the remaining sites did not have K_s values equal to or greater than 2.8 cm d^{-1}, there were no failing systems. It was hypothesized that the K_s was greater, in areas along the trench, than was measured. For example, at Sites B, C, D, and F, the K_s for either the horizontal or the vertically oriented samples were at or near the value that would be suitable (data not reported). In addition, K_s measured on small cores are typically less than K_s measured in boreholes because the large pores are cut and plugged by the cylindrical core. Thus, the soils may have percolation rates that are acceptable if they are measured in a borehole instead of cylindrical cores, but only marginally so.

K_{eff} of Biomat-affected Soil

Trench sidewall samples could not be sampled from Site A and G because the dispersal field had chambers which were impenetrable from the side. Consequently, only the natural vertical K_s and trench bottom K_{eff} could be compared for these two sites. There was no significant difference between the trench bottom and sidewall K_{eff} values (Table 3-4) for the remaining sites; thus, the K_{eff} values for the trench bottom and sidewall were averaged as one value for each site (Table 3-5).

The K_{eff} range for biomat-affected soils was 0.1 to 1.5 cm d^{-1} for Site A, B, C, D, and E, and 2.7 to 2.9 cm d^{-1} for Site F and G (Table 3-5). When comparing the natural soil (NS) and the biomat-affected soil (BS) within each site, Sites A, C, and G had significantly different K values (Table 3-6). Although the K_s and K_{eff} were significantly different in Site C, the K_s value for natural soil was less than the K_{eff} for the biomat-impacted soil. Because the natural soil K_s was less than the biomat-affected soil K_{eff} and they were significantly different, the biomat K_s could not be calculated for Site C. Site D did not show a statistical difference between the natural soil K_s and biomat-affected soil

K_{eff}, but the natural soil K_s was greater than the K_{eff} of the biomat-impacted soil. Sites E and F had smaller natural soil K_s values than the biomat-affected soil K_{eff}. Site F was hypothesized to have a large K_{eff} due to the abnormally high trench sidewall K_{eff} (Table 3-4). There was no significant difference between the natural soil K_s and biomat-affected soil K_{eff} of Sites E and F, thus it was deduced that the biomat K_s was the same as the natural soil K_s. The lack of reduction in K_s because of biomat formation at Sites C, E, and F, was interpreted to be from a number of reasons, including low K_s of the natural soils, natural variability in K_s, and variability in biomat development. Sampling active gravel-filled dispersal fields to obtain undisturbed samples was extremely tedious and minor disturbances may have occurred for part of the sample (Fig. 3-3).

Sites A and G had an 86 and 93% K_s reduction in the wastewater-impacted soils with biomats, while Site B and Site D had a 34 and 77% reduction in K_s, respectively (Table 3-6). There was no reduction of K_s for Sites E and F because the biomat K_s was deduced to be the same as the natural soil K_s. The hydraulic resistance for the natural soil of Sites A, B, D, and G ranged from 0.2 to 13.6 d, while the hydraulic resistance of the biomat-affected soil at these sites ranged from 2.3 to 95.1 d (Table 3-6). As the natural soil K_s decreased, the hydraulic resistance of biomat-affected soil increased. The hydraulic resistance of Magdoff and Bouma's (1975) sand textured soil with a biomat was 5.1 d, which is within the range of the biomat-affected soil's hydraulic resistance in this study. The hydraulic resistance of the natural soils at Sites C, E, and F ranged from 25.9 to 321.4 d, while the biomat-affected soil's hydraulic resistance ranged from 3.0 to 95.1 d (Table 3-6). Because these remaining sites did not have reduced K_s values, the hydraulic resistances of the biomat-affected soil did not increase; however, the range of hydraulic resistance was similar to the other sites (Sites A, B, D, and G).

The reductions of K_s (34 to 93%) for the biomat-affected soils at Sites A, B, D and G were smaller in this study than those reported in other studies (Jones and Taylor, 1965; Siegrist, 1987). Siegrist (1987) measured in-situ the hydraulic conductivity properties of a dispersal field located in silty clay loam textured soil with percolation rates ranging from 9 to 16 min cm^{-1}. The saturated hydraulic conductivity of the natural soil was 223 cm d^{-1} and dropped to <2.6 cm d^{-1} (99.5%) because of soil clogging after 2.5 yr of operation. Jones and Taylor (1965) measured the steady hydraulic conductivity rate, under continuous percolation for twenty weeks, of sand (coarse and fine) packed columns, overlain with gravel. The sand-textured soil K_s ranged from 610 to 1951 cm d^{-1} and reduced to 1.83 to 7.32 cm d^{-1} after biomat formation or 0.30% to 0.34% of the natural K_s. A smaller percentage reduction of K_s due to biomat formation in this study, as compared to that reported by others, was interpreted as caused by smaller K_s of the natural soils. For Site G, which had a sand texture, the K_s reduction caused by biomat formation was 93%.

Biomat thickness and Fabric

Visual estimates of the biomat thickness ranged from <0.1 to >3 cm (Figs. 3-4 and 3-5). Differences in biomat thickness resulted from system age, wastewater loading rates, system design, and the method of wastewater distribution. Installation imperfections also resulted in uneven wastewater loading; for example, the D-box at Site D was uneven causing unequal wastewater distribution. Serial wastewater distribution within the dispersal field also resulted in considerable differences in biomat thickness and hydraulic characteristics among the dispersal field trenches.

Quantitative measurements of biomat thickness from porosity evaluations indicated that the dark color used to estimate the biomat thickness at a macro-scale might overestimate the thickness of the biomat. The macro-scale measurements of the biomat thickness from Site C and E suggested the thickness was about 3 cm (Fig. 3-5). Other research studies (Jones and Taylor, 1965; Laak, 1970; Magdoff and Bouma, 1975; Siegrist, 1987; Thomas, 1966; Winneberger, 1984) reported the biomat thickness ranging from <0.5 cm to 4 cm. With closer inspection using fluorescence microscopy, the middle part of the dark layer at Site C had higher porosity than the upper and lower areas (Fig. 3-5, Right). The porous area within the dark layer suggested that the dark-colored layer was from staining of grain surfaces instead of pore filling (Fig. 3-5). The fabric and grain-size in the more porous area within the dark layer was different from the subsoil and was similar to fabric expected from a sand textured soil. The sandy fabric suggested that sand could have been placed in the trench bottom during dispersal field construction; although, the homeowners had indicated that this did not occur. Thus, it was hypothesized that high organic loading, constant saturation or near saturated conditions, and anoxic conditions may have induced the chemical reduction of Fe and Mn at the soil-trench interface. The effects of Fe and Mn being reduced are the production of protons that result in acidic conditions, which have been reported to dissolve clay and concentrate more resistant sand and silt (Brinkman, 1970). Reduction of the soil below the biomat was evident by the bluish-gray colors below the biomat-affected soil (Figs. 3-6 to 3-8).

Removal of Fe/Mn oxides and clay particles resulted in skeleton grains (sand) being more closely spaced than was observed in unaffected soil (Fig. 3-8).

Porosity measurements by image analysis indicated that only the upper few mm of the wastewater-impacted soil reduced pore area (Fig. 3-2). In addition, the pore size in the clogged zone was appreciably less than the underlying soil (Fig. 3-9). Biomat thickness ranged from 0.4 to 0.8 cm with an overall mean of 0.5 cm (Table 3-7). Siegrist (1987) reported a biomat thickness of <0.5 cm in soil cells treated with STE, which is within the range for this study. Thicker biomats, up to 3 cm, were reported by Magdoff and Bouma (1975).

Biomat K_s

Using the measured biomat thickness, hydraulic resistance, and K_{eff} of the biomat-affected soil, biomat K_s was calculated using Eq. [9]. The mean K_s of the biomat at Sites A, B, D, and G was 0.02, 0.12, 0.01, and 0.20 cm d^{-1}, respectively. Hydraulic resistance of the biomat was 15.6, 4.3, 81.5, and 2.2 d for Sites A, B, D, and G, respectively (Table 3-8). Sites E and F had a biomat K_s of 0.05 and 0.61 cm d^{-1} and a hydraulic resistance of 10.0 and 1.2 d. The hydraulic resistance increased as the K_s of the biomat decreased. Biomat K_s values reported by Keys et al. (1998) ranged from 0.02 cm d^{-1} for the bottom and sidewall areas to 2.41 cm d^{-1} for the unaffected upper sidewall. The biomat K_s values calculated in this study were within the K_s range reported by Keys et al. (1998).

Soil-Moisture Release Curve

For Sites D and E, van Genuchten parameters derived from the moisture release curves (Fig. 10) were similar for the natural and biomat-impacted soil (Table 3-9). The predicted van Genuchten parameters α and n for Site F were, however, significantly different. The biomat was thickest at this site (0.8 cm) which could result in the difference between the van Genuchten parameters; however, the hydraulic conductivities suggested there was no reduction in K_s from biomat formation. Therefore, the results from the van Genuchten predictions could also have been caused by natural soil K_s variability, low K_s of the natural soil, and sample disturbance when sampling gravel dispersal fields. The lack of measurable difference with and without the biomat should be expected. The volume of biomat-impacted soil in the cores was 25.4 to 50.9 cm^3 as compared to a total core volume of 572.6 cm^3. Thus, 4 to 9% of the soil volume evaluated was impacted by the biomat. Even if the van Genuchten's parameters for the biomat were different from those of the natural soil, the difference would probably not be measurable with the techniques used.

Conclusions

The K_s of the natural vertically and horizontally-oriented soil samples were not statistically different (α=0.10). The natural soil K_s ranged from <0.01 (Site B) to 41 cm d^{-1} (Site G) with two of the sites (A and G) having acceptable rates (>2.8 cm d^{-1}). The biomat-affected soil taken from the trench sidewall and bottom were also not statistically different (α=0.10), even though sidewall samples were taken above the trench bottom where biomat thickness would be expected to be less. The K_{eff} of the biomat-affected soil ranged from 0.2 (Site E) to 2.9 cm d^{-1} (Site G). The reduction in K_s occurred at four sites (Sites A, B, D, and G), reducing the K_s by 34 to 93%. The lack of reduction at the remaining sites was interpreted to be due to low K_s of the natural soil, natural variability in K_s, and variability in biomat development because of system design, system age, system installation, wastewater loading rates, and wastewater distribution.

Visual estimates of the biomat thickness ranged from <0.1 to >3 cm; however, biomat thicknesses ranged from 0.4 to 0.8 cm after quantitative measurements were made using fluorescence microscopy. The calculated biomat K_s ranged from 0.02 to 0.61 cm d^{-1} for Sites A, B, D, E, F, and G with hydraulic resistance ranging from 1.2 to 81.5 d. The biomat K_s was similar to the lower value (0.02 cm d^{-1}) reported by Keys et al. (1998). There was no statistical difference in van Genuchten's parameters at Site D and E, calculated from soil-moisture release curves, because the biomat volume was 4 to 9% the total volume of biomat-affected soil. There was a statistical difference at Site F; although, results from hydraulic conductivity measurements indicated no effect from biomat formation.

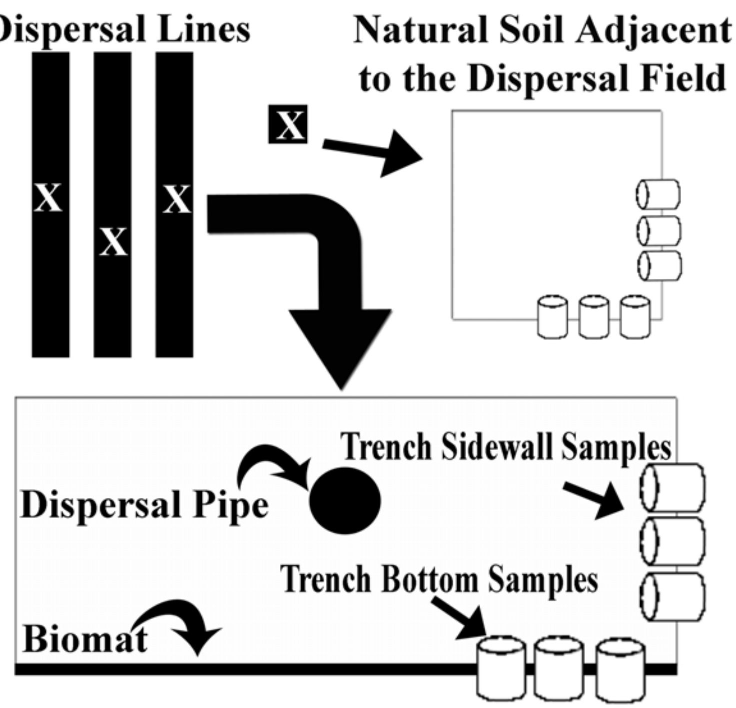

Figure 3-1. Method of sampling for biomat-affected soil and unaffected soil.

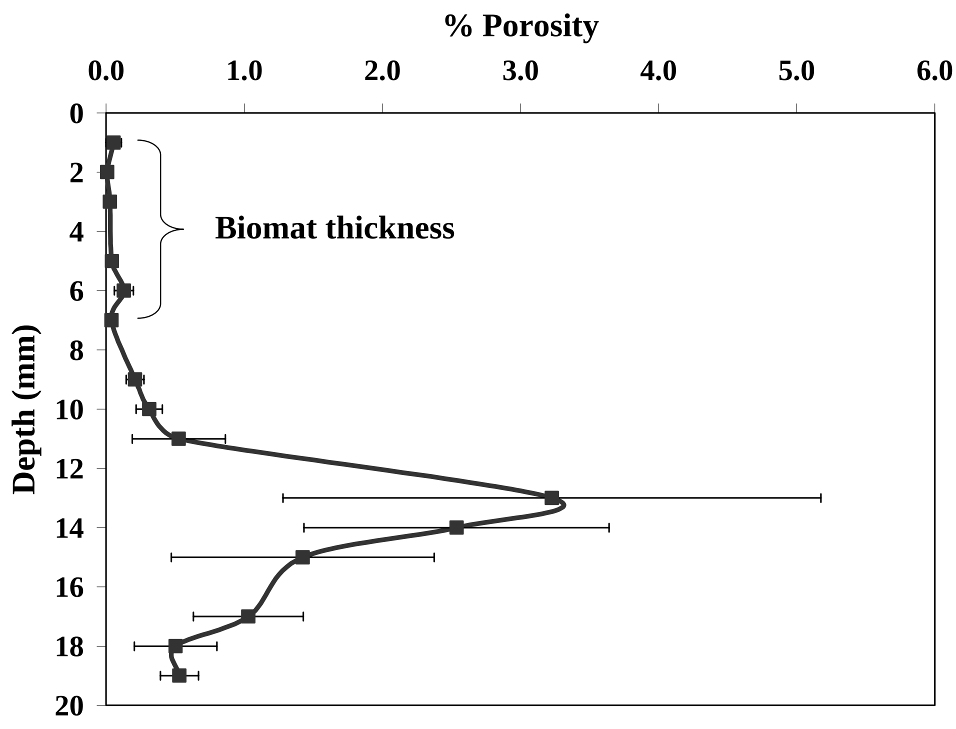

Figure 3-2. Percentage porosity with depth of polished block sample from Site C. The biomat was estimated to be 7 mm thick at this site.

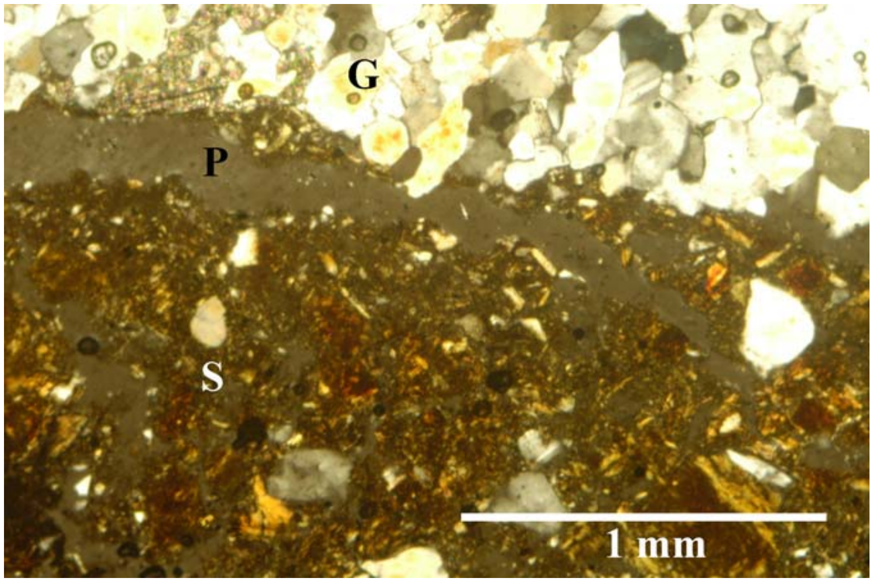

Figure 3-3. Thin-section of gravel piece above soil. Note crack between soil and overlying gravel that may indicate slight disturbances during sampling. G=gravel; S=soil; P=pore. Partially crossed polars.

Figure 3-4. Biomat from the trench bottom of Site A. Thickness of dark material is about 3 cm.

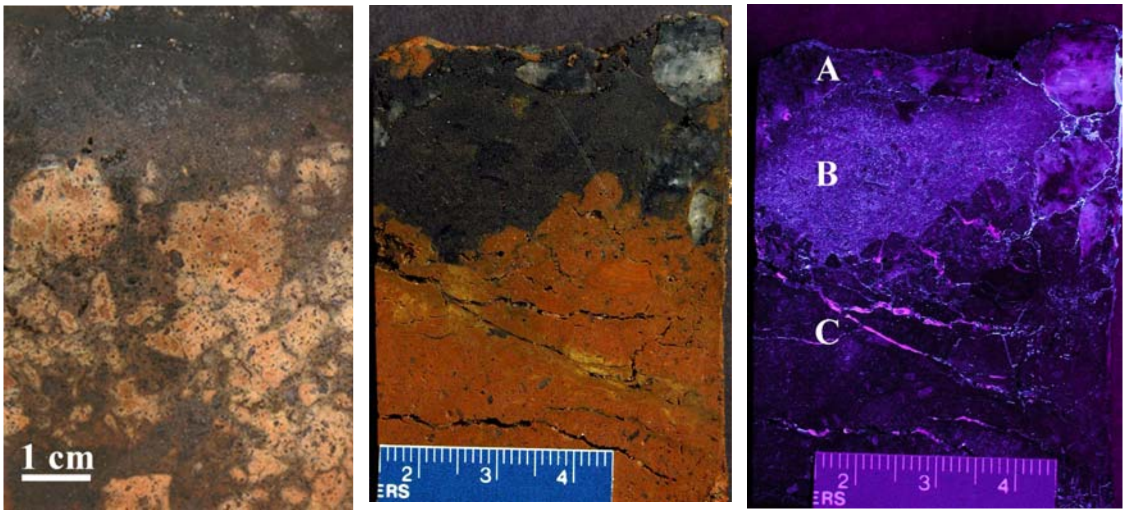

Figure 3-5. Polished blocks of trench bottom samples; Left-plane light image from Site E Middle-plane light image from Site C, Right-same view as left except photographed under UV light. A-biomat B-organic material coated grains C-subsoil. Scale in cm.

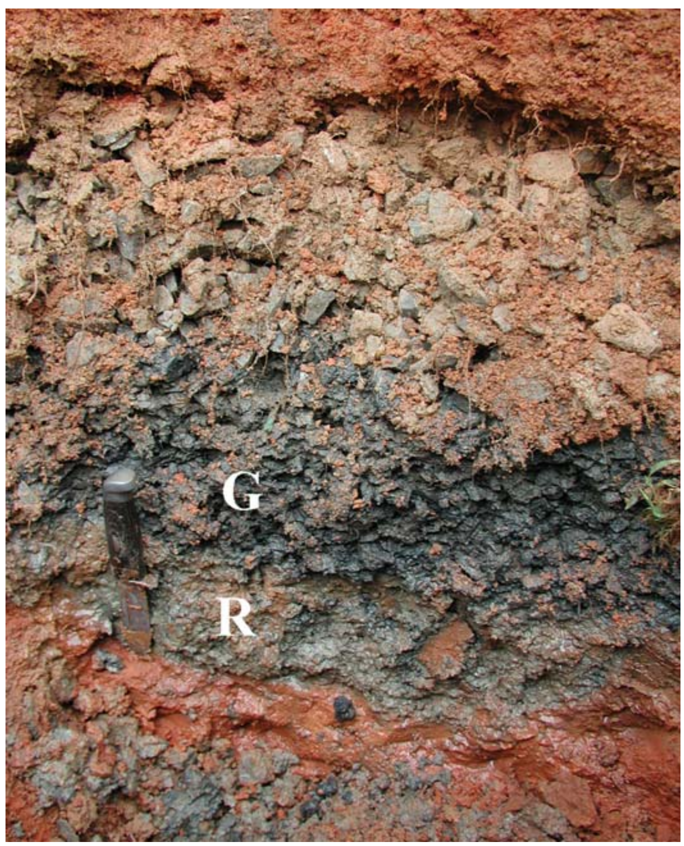

Figure 3-6. The trench bottom of Site E with biomat-coated gravel (G) and reduced soil below the biomat-affected soil (R).

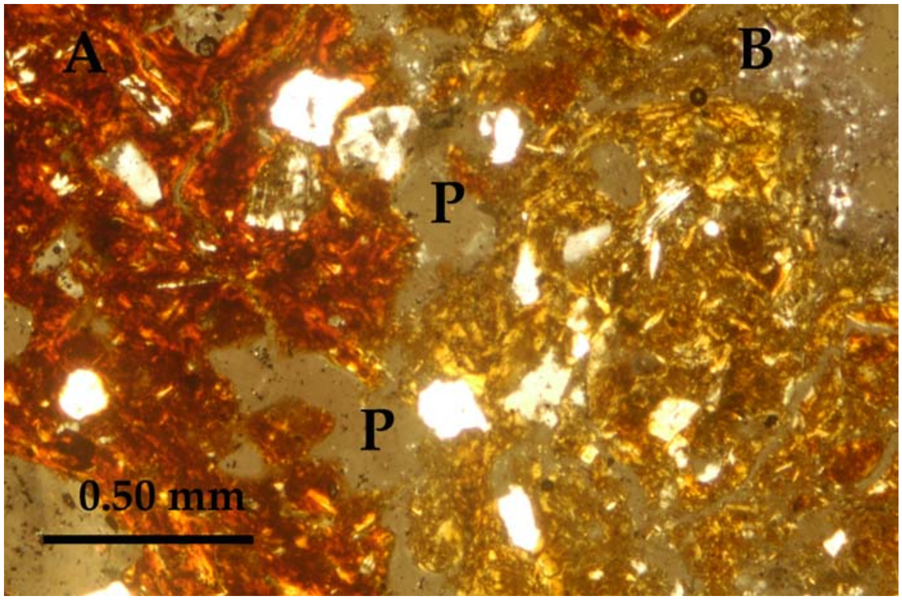

Figure 3-7. Thin-section of trench bottom samples from Site E. A-Red soil unaffected by wastewater application. B-Red Fe oxide coatings removed due to Fe reduction in the soil with presence of wastewater. P=pore, partially crossed polars.

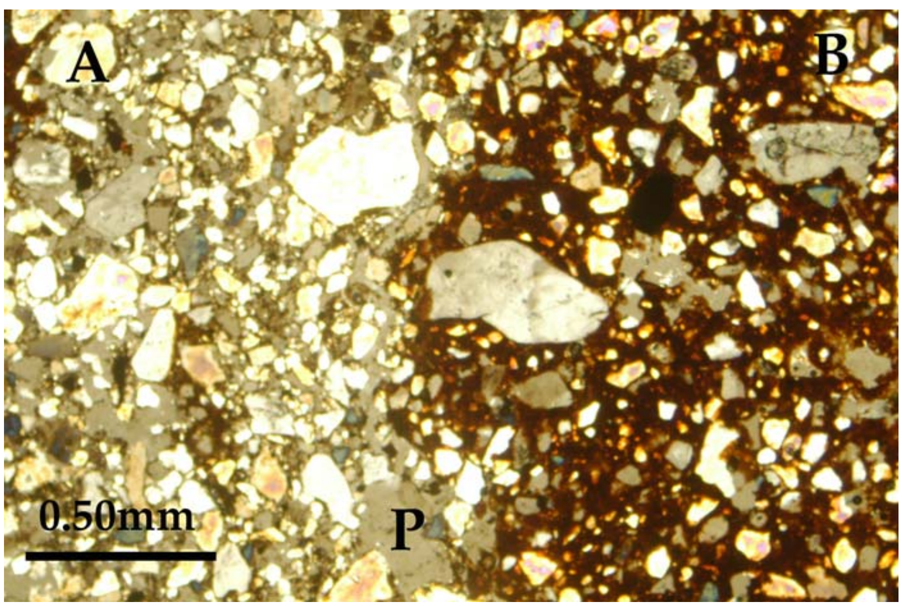

Figure 3-8. Reduction of Fe and Mn in trench bottom thin-section from Site D. A-gray soil reduced from Fe reduction and loss under the influence of wastewater. B-soil unaffected by wastewater. Note the closer placing of grains and less fine material in the gray zone. P=pores, partially crossed polars.

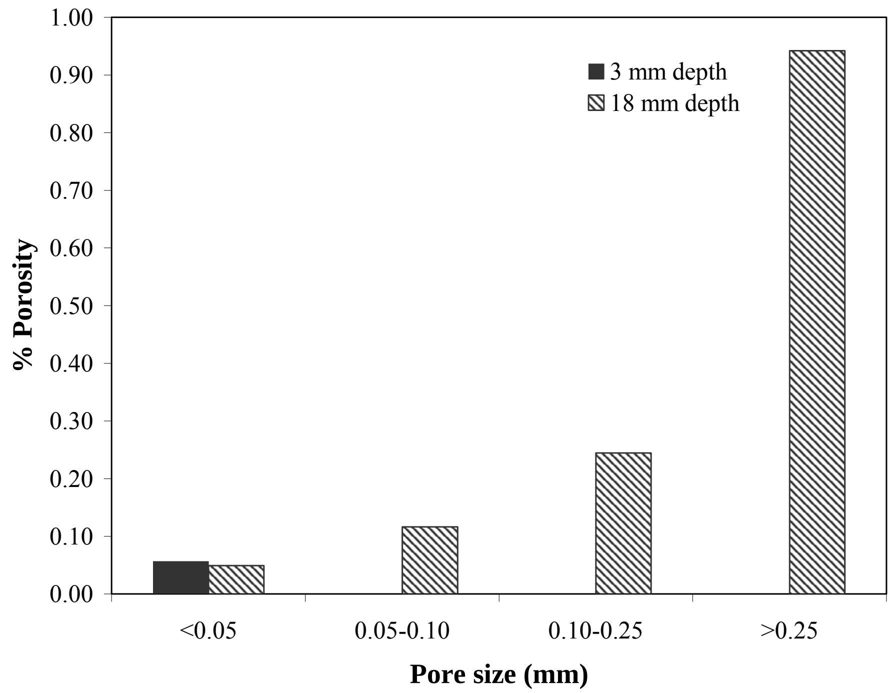

Figure 3-9. Pore size distribution at two depths in the biomat-affected soil at Site E. The biomat at this site is 3 mm thick. No pores >0.05 equivalent diameter were present in the biomat.

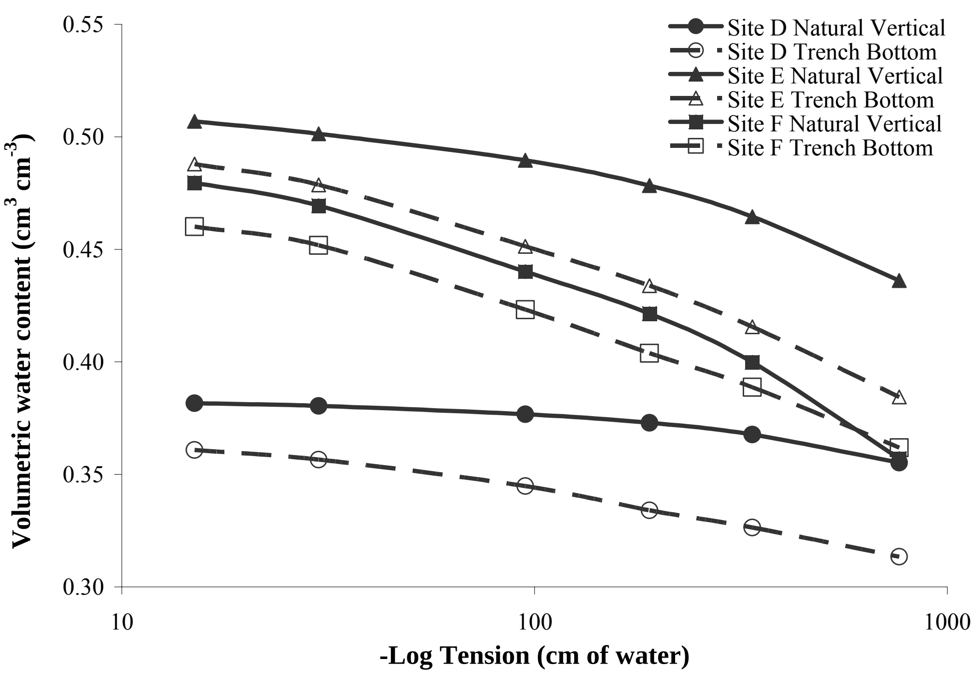

Figure 3-10. Soil-moisture release curve of natural vertical soil and trench bottom soil of Site D, E, and F. The volumetric water content of each site compared to the tension (log).

Table 3-1. Site Characteristics.

Site	Location	Age	Drain field design	Distribution Method	Number of bedrooms	Number of people
	County	y				
A	Forsyth	7	chamber	level field	3	NA†
B	Forsyth	7	EPS	serial	3	NA
C	Forsyth	43	gravel	serial	NA	8 to 9
D	Houston	13	gravel	d-box	4	3
E	Jackson	25	gravel	serial	3	4
F	Baldwin	10	gravel	serial	4	6
G	Jeff Davis	10	chamber	one line	3	2

† Houses were recently abandoned due to property sale.

Table 3-2. Geometric mean of effective saturated hydraulic conductivity of natural soil in vertical (NV) and horizontal (NH) orientation.

Site	Soil Type	Mean
		$cm\ d^{-1}$
A	NV	3.16
	NH	NA‡
B	NV	1.25a†
	NH	0.94a
C	NV	0.03a
	NH	0.02a
D	NV	0.16a
	NH	1.08a
E	NV	0.08a
	NH	0.05a
F	NV	0.48a
	NH	0.67a
G	NV	40.98
	NH	NA

† Means followed by the same letter are not significantly different within sites at α=0.10.
‡ Because the trench sidewall samples could not be collected from chamber systems, horizontally oriented natural soil samples were not collected.

Table 3-3. Geometric mean K_s for natural soil.

Site	Texture	Mean K_s
		cm d^{-1}
A	cl§	3.2(0.3)†b‡
B	l	1.1(0.3)bc
C	c	0.0(0.3)f
D	sc	0.4(0.3)cde
E	c	0.1(0.3)def
F	scl	0.6(0.5)cd
G	s	41.0(0.1)a

† Standard error of the mean is in parenthesis.
‡ Means followed by the same letter are not significantly different between sites at α=0.10.
§ cl=clay loam, l=loam, c=clay, sc=sandy clay, scl=sandy clay loam, and s=sand

Table 3-4. Geometric mean of effective saturated hydraulic conductivity of trench bottom (TB) and trench sidewall (TS).

Site	Soil Type	Mean
		cm d^{-1}
A	TB	0.45
	TS	NA
B	TB	1.00a‡
	TS	0.68a
C	TB	1.78a
	TS	1.23a
D†	TB	0.11a
	TS	0.08a
E	TB	0.14a
	TS	0.64a
F	TB	1.38a
	TS	10.58a
G	TB	2.91
	TS	NA

† No visual indication of biomat formation.
‡ Means followed by the same letter are not significantly different within sites at α=0.10.

Table 3-5. Geometric mean K_{eff} for biomat-affected soil.

Site	Texture	Mean K_{eff}
		cm d^{-1}
A	cl§	0.5(0.4)†bcde‡
B	l	0.8(0.2)bcd
C	c	1.5(0.1)abc
D	sc	0.1(0.3)def
E	c	0.2(0.5)def
F	scl	2.7(0.4)ab
G	s	2.9(0.2)a

† Standard error of the mean is in parenthesis.
‡ Means followed by the same letter are not significantly different between sites at α=0.10.
§ cl=clay loam, l=loam, c=clay, sc=sandy clay, scl=sandy clay loam, and s=sand

Table 3-6. Geometric mean of effective saturated hydraulic conductivity of natural soil (NS) and biomat-affected soil (BS), hydraulic resistance, and percent of reduction. α=0.10

Site	Texture	NS Mean K_s	Resistance of NS	BS Mean K_{eff}	R of BS	K Reduction
		cm d^{-1}	d	cm d^{-1}	d	%
A	cl	3.2(0.3)†a§	2.4	0.5(0.4)b	18.0	86
B	l	1.1(0.3)a	7.1	0.7(0.2)a	11.3	34
C	c	0.0(0.3)a	321.4	1.5(0.1)b	5.8	NA‡
D	sc	0.4(0.3)a	13.6	0.1(0.3)a	95.1	77
E	c	0.0(0.3)a	213.4	0.1(0.5)a	95.1	0
F	scl	0.3(0.5)a	25.9	2.7(0.4)a	3.0	0
G	s	41(0.1)a	0.2	2.9(0.2)b	2.3	93

† Standard error is in parenthesis.
‡ Percent reduction could not be calculated because NS<BS.
§ Sites with the same letter indicate no significant difference between the NS and BS within the site at α=0.10.

Table 3-7. Biomat thickness of trench bottom and trench sidewall derived from the porosity measurements of polished block samples.

	Trench Bottom		Trench Sidewall		Mean
Site	Thickness	n	Thickness	n	Thickness
	cm		cm		cm
A	0.4(0.12)†	3	NA‡	NA	0.4(0.12)
B	0.4(0.10)	2	0.6(0.10)	2	0.5(0.08)
C	0.5(0.20)	2	0.7	1	0.6(0.13)
D	0.6(0.05)	2	0.6	1	0.6(0.03)
E	0.5(0.09)	7	0.3	1	0.5(0.08)
F	0.8(0.55)	2	NA	NA	0.8(0.55)
G	0.4(0.05)	10	NA	NA	0.4(0.05)
Total Mean	0.5(0.05)		0.6(0.07)		0.5(0.04)

† Standard error is in parenthesis.
‡ Sidewall samples could not be sampled at Sites A and G because of chamber systems and the sidewall samples at Site F were damaged during polished block preparation.

Table 3-8. Biomat hydraulic resistance and K_s.

Site	R of biomat	Biomat K_s
	d	cm d^{-1}
A	15.6	0.02
B	4.3	0.12
D	81.5	0.01
E	10.0	0.05
F	1.2	0.61
G	2.2	0.20

Table 3-9. Van Genuchten's parameters for the natural vertical and trench bottom samples of Site D, E, and F.

Site	Soil Type	θ_s	θ_r	α	n
		-------------cm^3 cm^{-3}----------		-1 cm^{-1}	
D	NS	0.39a†	0.10a	0.07a	1.04a
	BS	0.41a	0.08a	0.10a	1.06a
E	NS	0.48a	0.10a	0.04a	1.08a
	BS	0.50a	0.10a	0.03a	1.10a
F	NS	0.52a	0.10a	0.02a	1.15a
	BS	0.50a	0.09a	0.42b	1.09b
Mean		0.45	0.09	0.07	1.09

† Sites with the same letter indicate no significant difference between the NS and BS within the site at α=0.05.

References

Bouma, J. 1975. Unsaturated flow during soil treatment of septic tank effluent. J. Environ. Eng. Div. Am. Soc. Civ. Eng. 101: 967-983.

Beach, D.N.H., and J.E. McCray. 2003. Numerical modeling of unsaturated flow in wastewater soil absorption systems. Ground Water Monit. Remediation 23:64-72.

Brinkman, R. 1970. Ferrolysis, a hydromorphic soil forming process. Geoderma. 3:199-206.

Burke, W., D. Gabriels, and J. Bouma. 1986a. Structural state parameters. p. 23-42. *In* Soil structure assessment. A.A. Balkema, Rotterdam, Netherlands.

Burke, W., D. Gabriels, and J. Bouma. 1986b. Water and air flow parameters. p. 43-71. *In* Soil structure assessment. A.A. Balkema, Rotterdam, Netherlands.

Collins, T. 2005. Image J. Image processing and analysis in Java. [Online]. Available at http://www.uhnresearch.ca/facilities/wcif/imagej/ (verified 08 Nov. 2005).

Dane and Hopmans, 2002. Pressure cell. p. 684-688. *In* J.H. Dane and G.C. Topp (ed.) Methods of soil analysis. Part 4. SSSA, Inc., Madison, WI.

Georgia Dep. of Human Resources. 1998. Manual for on-site sewage management systems. Georgia Dep. of Human Resources, Atlanta, GA.

Gray, N.F. 2004. Biology of wastewater treatment. 2nd ed. Imperial College Press, London.

Gerardi, M.H. and M.C. Zimmerman. 2005. Wastewater pathogens. Wiley-Interscience, Hoboken, N.J.

Hillel, D. 1998. Environmental soil physics. Academic Press, USA.

Jones, J.H. and G.S. Taylor. 1965. Septic tank effluent percolation through sands under laboratory conditions. Soil Sci. The Williams and Wilkins Co., USA.

Keys, J.R., E.J. Tyler, and J.C. Converse. 1998. Predicting life for wastewater absorption systems. p. 167-176. *In* Proc. of the Eighth Natl. Symp. on Individual and Small Community Sewage Systems, 8th, Orlando, FL, USA. 8-10 Mar. 1998. ASAE Publ. 10-91:192-200. St. Joseph, MI.

Kilmer, V.J. and L.T. Alexander, 1949. Methods of making mechanical analysis of soil. Soil Sci. Soc. Am. J. 68: 15-24.

Klute, A. and C. Dirksen. 1986. Hydraulic conductivity and diffusivity: Laboratory methods. p. 687-734. *In* A. Klute (ed.) Methods of soil analysis. Part 1. 2nd ed. Agron. Monogr. 9 ASA and SSSA, Madison, WI.

Laak, R. 1970. Influence of domestic wastewater pretreatment on soil clogging. J. Water Pollut. Control Fed. Part I. 42:1495-1500.

Magdoff, F. R. and J. Bouma. 1975. The development of soil clogging in sands leached with septic tank effluent. p. 37-47 *In* Proc. of the Natl. Home Sewage Disposal Symp. ASAE Publ. Chicago, USA. 9-10 Dec. 1974. St. Joseph, MI.

McLean, E.O. 1982. Soil pH and lime requirement. p. 199-223. *In* A.L. Page (ed.) Methods of soil analysis. Part 2. 2nd ed. Agron. Monogr. 9 ASA and SSSA, Madison, WI.

Murphy, C.P. 1986. Thin section preparation of soils and sediments. A B Academic Publishers. Berkhamsted, Great Britain.

Radcliffe, D.E. and L.T. West. 2000. Relating saturated hydraulic conductivity to percolation and borehole permeameter tests. Soil Survey Hor. 41:99-103.

Siegrist, R.L. 1987. Soil clogging during subsurface wastewater infiltration as affected by effluent composition and loading rate. J. Environ. Qual. 16:181-187.

Stoops, G. 2003. Guidelines for analysis and description of soil and regolith thin sections. SSSA, Inc. Madison, WI, USA.

Thomas, R.E., W.A. Schwartz, and T.W. Bendixen. 1966. Soil chemical changes and infiltration rate reduction under sewage spreading. Soil Sci. Soc. Am. Proc., 30:641-646.

U.S. Census Bureau. 1990a. Housing Characteristics. [Online]. Available at http://factfinder.census.gov/servlet/QTTable?_bm=y&-state=qt&-context=qt&-qr_name=DEC_1990_STF3_DP5&-ds_name=DEC_1990_STF3_&-CONTEXT=qt&-tree_id=100&-all_geo_types=N&-redoLog=true&-geo_id=01000US&-geo_id=04000US13&-search_results=01000US&-format=&-_lang=en (posted 1 April 1990; verified 11 Dec. 2005).

U.S. Census Bureau. 2000b. General Housing Characteristics. [Online]. Available at http://factfinder.census.gov/servlet/QTTable?_bm=y&-context=qt&-qr_name=DEC_2000_SF1_U_QTH1&-ds_name=DEC_2000_SF1_U&-CONTEXT=qt&-tree_id=4001&-all_geo_types=N&-redoLog=true&-_caller=geoselect&-geo_id=01000US&-geo_id=04000US13&-search_results=01000US&-format=&-_lang=en (posted 1 April 2000; verified 12 Dec. 2005).

USEPA. 2002. On-site wastewater treatment systems manual. EPA/625/R-00/008 Office of Water. Office of Research and Development. (Available on-line http://www.epa.gov/ORD/NRMRL/Pubs/625R00008/625R00008.pdf.) (Verified 13 Aug. 2002.)

White, K.D. 2002. Evaluation of the hydraulic conductivity of EZ flow brand hardened expanded polystyrene aggregate as compared to gravel systems. [Online].

White, K.D. and L.T. West. 2003. In-ground dispersal of wastewater effluent: The science of getting water into the ground. Small Flows Quarterly. 4 vol. no. 2

Winneberger, J.H.T. 1984. Septic-tank systems: A consultant's toolkit. Butterworth, Stoneham, MA.

CHAPTER 4

MODELING TWO-DIMENSIONAL FLOW FROM OWMS DISPERSAL FIELDS IN A CLAY LOAM AND SAND TEXTURED SOIL

Introduction

A software package known as Hydrus-2D can be used to model two-dimensional water flows in variably saturated media by specifying the soil's hydraulic parameters (e.g. K_s for specified textures, etc.) (Šimůnek et al., 1998). Because there is no analytical solution to the Richards (1931) equation for unsaturated flow, using numerical models are very useful tool. Using the hydraulic and physical characteristics of the natural soil and biomat in OWMS, Hydrus-2D can better simulate real dispersal field flows.

Limited studies have used Hydrus-2D to simulate dispersal field flows (Beach and McCray, 2003; Radcliffe et al., 2005). Beach and McCray (2003) modeled two-dimensional flow in OWMS in a sand-and a silt textured soil. The natural sand and silt soil had a K_s of 2000 and 40 cm d^{-1}. The sand and silt textures with shallow ponding (4 to 10 cm) had bottom and sidewall K_{eff} values of 6.0 cm d^{-1} and 7.44 cm d^{-1}, while the K_{eff} for the trench bottom and sidewall was 1.5 cm d^{-1} and 2.16 cm d^{-1} for coarse sand and silt textures with deep ponding (20 to 23 cm). The results from the models indicated that the hydraulic properties of the clogging zone and subsoil contributed to the flow rate and water content distributions within the OWMS (Beach and McCray, 2003).

The average linear water velocity and hydraulic resistance for a shallow ponded trench bottom with sand textured soil was 29 cm d^{-1} and 2.1 d, while the deep ponded system was 25 cm d^{-1} and 2.4 d. The increased hydraulic resistance in the sand systems resulted in decreased water content throughout the system and increased the wastewater treatment area. The silt trench bottom with shallow ponding had a linear water velocity and hydraulic resistance of 22 cm d^{-1} and 2.7 d and the deep ponding trench bottom had 15 cm d^{-1} and 4.0 d. The silt system had substantially greater residence times than the sand system because of lower overall unsaturated hydraulic conductivity. Increased hydraulic resistance for both sand and silt systems increased sidewall flow (Beach and McCray, 2003). Because hydraulic residence times are generally correlated to purification processes, the increase from the degree of clogging can be seen as potential enhancement in wastewater treatment.

Radcliffe et al. (2005) modeled flow through the trench bottom consisting of a BC and Bt1 horizon in a Cecil soil. The biomat thickness was 2 cm with K_s of 0.05 cm d^{-1} and the level of water in the trench was arbitrarily set at 5 cm. The BC horizon had a natural soil K_s was 0.84 cm d^{-1} and the Bt1 horizon K_s was 257.5 cm d^{-1}. Five models were tested per horizon to compare wastewater infiltration rates of an open trench to trenches with gravel masking, embedded gravel, and sidewall flow for the open trench and embedded gravel. There was a small effect from gravel masking in the BC horizon, because there was a large gradient at the soil surface next to the gravel particles that pulled the water laterally beneath the gravel. The embedded gravel had a greater effect in reducing infiltration rates (ratio of open trench to gravel of 1.5). When sidewall was included in the open trench and embedded gravel system, the total infiltration rates increased for each system. The open trench infiltration rate increased from 0.31 to 0.43

cm d^{-1} and was 1.33 times greater than the embedded gravel system, while the embedded gravel system's infiltration rate increased from 0.21 to 0.32 cm d^{-1}.

The infiltration rates were higher in the Bt1 horizon than in the BC horizon. The open system infiltration rate was 1.34 times greater than the gravel-masked system and 1.93 times greater than the embedded gravel system. When sidewall flow was included, the infiltration rate in the open system increased from 0.75 to 1.04 cm d^{-1} and was 1.7 times greater than the embedded gravel system. The embedded gravel system's infiltration rate increased from 0.39 to 0.61 cm d^{-1}. Sidewall flow allowed more infiltration in both horizons and reduced the affect of the embedded gravel. Radcliffe et al. (2005) results indicated that there was a greater impact on infiltration rates when there is a large difference between the biomat K_s and the natural soil K_s.

The objective of this study was to evaluate the trench bottom and sidewall flow from mature dispersal fields in sand and clay loam textured soil using two-dimensional models. Another objective was to develop a method of allowing the level of water in the trench to vary in response to the dosing rate into the trench and flow out of the trench through the bottom and sidewall.

Materials and Methods

Field Methods

Two OWMS sites were selected from the previous study in Chapter 3, one in the Georgia Piedmont (Forsyth County) and the second in the Coastal Plain (Jeff Davis County) for model simulations. The Piedmont dispersal field (Site A) was 7-yr-old and had a chamber system with the trench bottom placed in a clay loam textured BC2 horizon. The Coastal Plain dispersal field (Site G) was also a chamber system and 10-yr-old with the trench bottom located in a sand textured Bh horizon. Measurements of particle size distribution, bulk density, and saturated hydraulic conductivity of the natural soil and biomat are reported in Chapter 3.

Model Simulation Methods

Hydrus-2D, a numerical simulation model, was used to model two-dimensional water flow because it can simulate the movement of water, heat, and solutes in variably saturated soil (Šimůnek et al., 1998). One-half of the dispersal field was used for simulations, assuming the middle of the trench would be an axis of symmetry. The dispersal field configuration used for model simulations was a 45 cm wide (half that of a full trench) and 31 cm deep gravel trench with the water table 60 cm below the trench bottom (Fig. 4-1). For initial conditions, the soil profile was in equilibrium with the water table (190 cm below the soil surface). The trench bottom was 130 cm below the soil surface and the width of the model space from the center of the trench was 180 cm to the right. The model space width (180 cm) was chosen to ensure that the soil boundary did not interfere with water flow. The trench was aggregate filled with a distribution pipe 22 cm from the trench bottom. The trench bottom and sidewall biomat thickness was 3 cm, with the sidewall biomat extending to a height of 11 cm above the trench bottom (Fig. 4-1). Although measurements indicated the biomat thickness in these soils was less than 0.8-cm thick, a biomat thickness of 3 cm was used for model simulations in order to increase the number of nodes within the biomat (Fig. 4-1). By increasing the number of nodes in the biomat, accuracy in predicting wastewater flows increased. The biomat K_s was increased from that measured at the sites such that the biomat hydraulic resistance remained the same as that measured for the sites (Table 4-1).

The flow (Q) per day through the trench bottom and trench sidewall was evaluated per cm of trench length (units of $cm^3\ cm^{-1}\ d^{-1} = cm^2\ d^{-1}$). Flows were also evaluated for the top of the trench and the biomat-affected sidewall (lower 11 cm of the sidewall). The wastewater loading rate was 2 cm d^{-1} applied in three equal doses during the day at 0800 h, 1400 h, and 2000 h for Site A and 4 cm d^{-1} for Site G. Dosing times were chosen from the frequency pattern of a single-family residence (USEPA, 2002). Each dose lasted 48 min. The loading rates are typical loading rates used for soils with properties similar to these in Georgia (USEPA, 2002).

Water retention parameters and hydraulic conductivities for the simulations were predicted using Hydrus-2D's neural network. Particle size distribution, bulk density, and K_s measured for the sites were input and van Genuchten's parameters (n, α, θ_s, θ_r) were derived by the model (Table 4-1). For the aggregate in the trench, we used van Genuchten parameters that would result in a very steep moisture release curve, a very high K_s (1000 cm d^{-1}), a very low residual water content (θ_r=0.05), and a saturated water content based on half the pore space being filled with aggregate (θ_s=0.50).

There were four model simulations. One simulation for each site had the same K_s for the trench bottom and trench sidewall. The other two simulations assumed that the sidewall biomat K_s was twice that of the trench bottom (Table 4-1). Model simulations were run until total outflow reached steady state, which required 13 d.

Results and Discussion

Soil Moisture Release

The van Genuchten parameters predicted by Hydrus-2D for Site A were compared to the predicted parameters (Table 3-9, Chapter 3) of three OWMS in the

Georgia Piedmont (Sites D, E, and F). In general, the predicted parameters were similar to those measured. The greatest difference between measured and predicted values was for n and α (Table 4-1).

Dispersal Fields in Clay Loam Soil

The total trench output for the clay loam soil with equal trench bottom and trench sidewall biomat K_s was 88.5 cm^3 cm^{-2} d^{-1} which was 98.3% of the total input of 90 cm d^{-1} (Table 4-2). Ponding depths at steady state were 10.3, 10.9, and 11.2 cm for the dosing times at 0800 h, 1400 h, and 2000 h, respectively (Fig. 4-2). The minimum ponding depth prior to the 0800 h dose was 9.4 cm; thus, flow through the trench bottom varied only slightly due to the increased head associated with each dose (Fig. 4-2 and 4-3). Most of the variation in total outflow due to each dose application was from differences in sidewall flow (Fig. 4-4).

The majority of the flow, 62.0 cm^3 cm^{-2} d^{-1} (68.9%), was through the trench bottom, while 26.5 cm^3 cm^{-2} d^{-1} (29.4%) was through the trench sidewall (Fig. 4-3 and Table 4-2). The flow through biomat-affected sidewall was 14.5 cm^3 cm^{-2} d^{-1} (16.1% of the total flow), while the flow above the biomat was 12.0 cm^3 cm^{-2} d^{-1} (13.3%) (Table 4-2). Most of the increased sidewall flow associated with dose application was through soil above the biomat-impacted sidewall. Sidewall flow above the biomat, reported by Keys et al. (1998), for a sand textured soil was 2.41 cm d^{-1}. This value is much higher than the flow rate simulated in this study (0.27 cm d^{-1}), which was expected because soils with a high percentage of sand have higher soil K_s. As ponding height decreases between doses, flow continues in the zone just above the biomat although wastewater ponding height is below this level (Figs. 4-4 and 4-5B). This flow may also be an artifact of the moisture release characteristics of the simulated media filling the trench (Table 4-1). Ideally, the moisture release curve should be flat and equal to the water content for all negative pressures and rise to saturation abruptly at positive pressures. This would require α to be very large. We used the largest value of α that resulted in accurate model runs (α=1, Table 4-1). However, large values of α caused the numerical solution not to converge. This artifact would not be expected to appreciably affect relative total daily flow through the trench bottom and sidewall.

The clay loam system with the biomat sidewall K_s 2 times greater than the bottom biomat K_s had a total outflow of 88.0 $cm^3\ cm^{-2}\ d^{-1}$ which was 97.8% of total inflow (Fig. 4-6 and Table 4-2). A majority of flow, 60.0 $cm^3\ cm^{-2}\ d^{-1}$ (66.7%), was through the trench bottom and the remaining flow, 28.0 $cm^3\ cm^{-2}\ d^{-1}$ (31.1%), was through the trench sidewall. There was a higher percentage of flow through the sidewall as compared to the clay loam simulation with equal trench bottom and trench sidewall biomat K_s, which was expected because the biomat-affected sidewall had a higher K_s. Because the K_s of the sidewall biomat was 2 times the clay loam soil with equal trench bottom and sidewall K_s, the flow through the biomat-affected sidewall was about 2 times greater (Table 4-2). The maximum ponding depths were 9.4, 9.9, and 10.3 cm for the daily doses (Fig. 4-7). Because ponding never reached 11 cm, there was no flow above the biomat-affected sidewall. The change in the trench bottom flow was only 2.2% less than the other system that was caused by more flow being accepted through the biomat-affected sidewall.

When comparing the flows of the clay loam models from time zero days to the time the flows reached steady state (13 d), slight differences in the total flows can be observed (Fig. 4-8). The clay loam soil with trench sidewall biomat K_s twice that of the bottom biomat K_s had higher initial flows than the other clay loam model before reaching steady state. This resulted from the biomat-affected sidewall biomat K_s being 2 times greater than the other clay loam system's sidewall biomat K_s. As wastewater ponding became steady, the ponding heights were greater and the clay loam system with equal trench sidewall and bottom biomat K_s had higher peak flows associated with each dose because 45% of total sidewall flow was being accepted by the unaffected trench sidewall.

The model predicted that a very small amount of the total outflow (< 1%) was through the top of the trench. This small flow may be an artifact of the characteristics of the simulated material filling the trench. The trench sidewall flows in this study (0.32 to 0.62 cm d^{-1}) are similar to the trench sidewall flows (0.17 to 0.62 cm d^{-1}) of the clay textured soil reported by Bouma (1975). Trench bottom flows (0.17 to 0.75 cm d^{-1}) were much lower in Bouma's (1975) study.

Dispersal Fields in Sand Soil

Of the 180 cm d^{-1} applied to both the sand textured system, 99.8% of the flow was accepted by the trench bottom when at steady state (Table 4-2). The high acceptance by the trench bottom was due to the high K_s of the natural soil. Unlike Bouma (1975), there was no sidewall flow and the flows of the trench bottom were less than his reported values (5.8 to 7.5 cm d^{-1}). This is attributed to the higher K_s (~550 cm d^{-1}) of Bouma's (1975) sand.

The soil closest to the dispersal line had the most wastewater contact (ponding depth of 3.8 cm) and decreased to unsaturated conditions before reaching the sidewall (Fig. 4-8). A shorter dosing period (< 48 min) was expected to increase ponding depth and wastewater treatment area, but was not expected to appreciably impact results since most flow would be through the trench bottom. Because 99.8% of the flow was accepted by the trench bottom closest to the dispersal line (trench bottom), no sidewall flow occurred (Fig. 4-9). There is a lag time between when wastewater is dosed and when ponding occurs. At 0824 h (13.35 d), ponding begins at the trench bottom even though dosing began at 0800 h (Fig. 4-8). After each dose, it took on average 25 min for ponding to occur. The ponding height and flow closest to the trench increased after each dose (Fig. 4-9). After the third dose, the highest ponding depth occurred (3.8 cm) at 2136 h (13.9 d) (Fig. 4-8). Wastewater ponding began to decrease at 2400 h (14.0 d) and reached unsaturated conditions at 0224 h (14.1 d) (Fig. 4-8). Total flow and pressure heads (cm) decreased during the resting periods after each dose (Fig. 4-9). These results were the same for the dispersal field in sand textured soil with a sidewall biomat K_s being 2 times the trench bottom biomat.

The sand-textured soil flow simulations reached steady state (2 d) much faster than the clay loam flow simulations (13 d) which was due to the sand K_s being greater than the clay loam K_s (Fig. 4-11).

Conclusions

For both simulations in the clay loam soil, there was greater trench bottom flow (66.7 to 68.9%) than the sidewall flow (29.4 to 31.1%). With the trench sidewall biomat K_s twice that of the bottom biomat K_s, ponding decreased and sidewall flow occurred only through the biomat-affected sidewall. The lower trench bottom flow with equal bottom and sidewall biomat K_s was attributed to more flow acceptance by the biomat-affected sidewall. Because the sidewall became unsaturated above the resting ponding depth, the sidewall had sharper increases in flow, after dosing, than the trench bottom.

The trench sidewall flows in this study (0.32 to 0.62 cm d^{-1}) were similar to the trench sidewall flows (0.17 to 0.62 cm d^{-1}) of the clay textured soil reported by Bouma (1975). The trench bottom flows (0.17 to 0.75 cm d^{-1}) were much lower in Bouma's (1975) study.

Both sand-textured simulations had 99.8% of flow accepted by the trench bottom. Soil closest to the dispersal pipe accepted the wastewater flow, while the total sidewall and half the trench bottom remained unsaturated. Bouma (1975) reported higher flows for the trench bottom (5.8 to 7.5 cm d^{-1}) than the values reported in this study, which was attributed to the higher natural soil K_s.

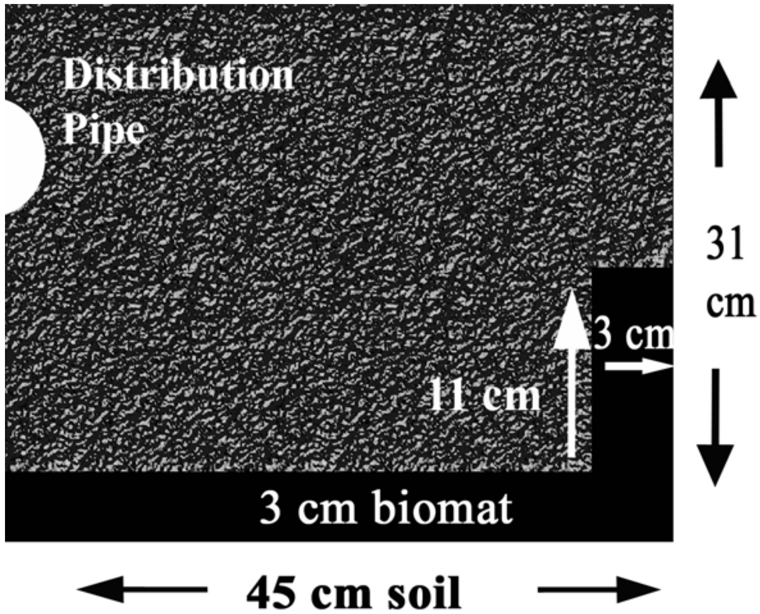

Figure 4-1. Half the dispersal trench used for model simulations.

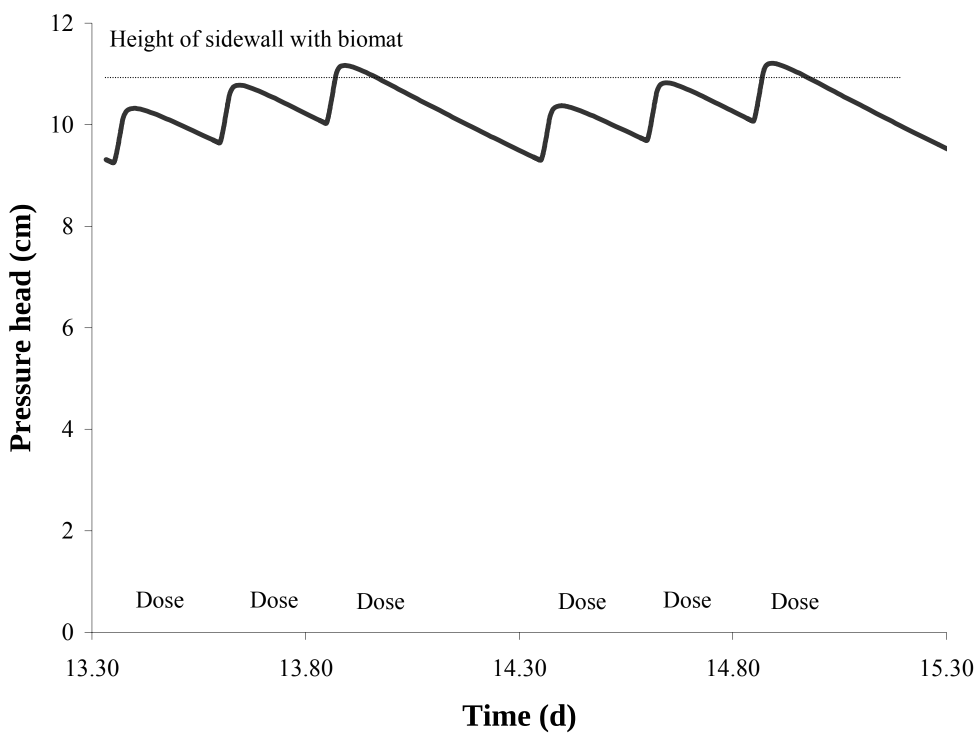

Figure 4-2. Pressure head (cm) of dispersal field in clay loam soil with equal trench bottom and sidewall K_s.

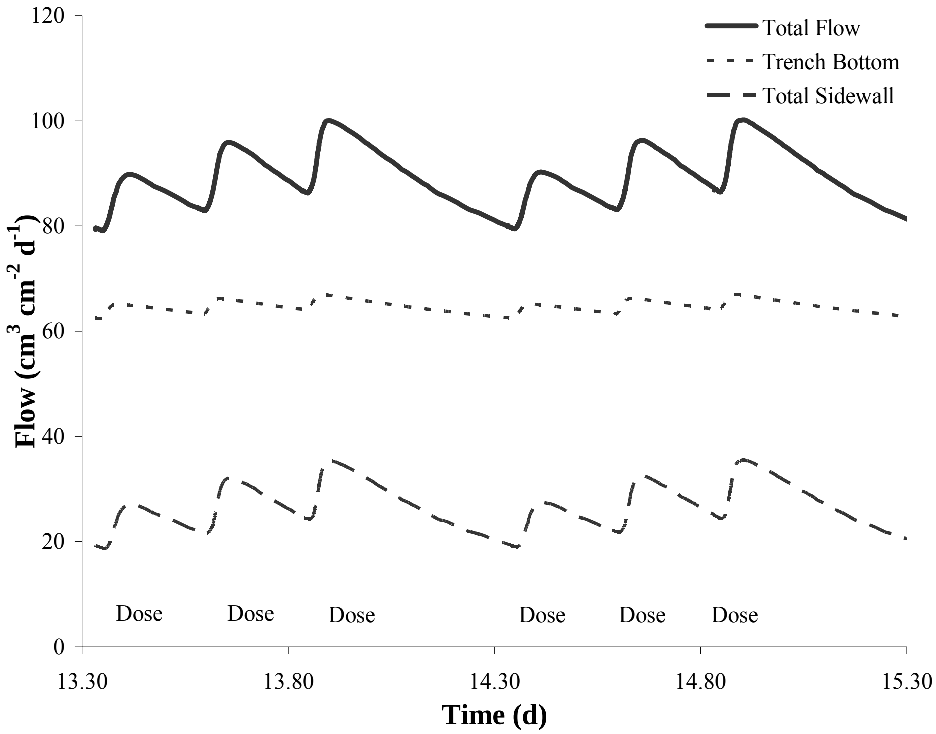

Figure 4-3. Total system, trench bottom, and sidewall flow of dispersal field in clay loam soil with equal trench bottom and sidewall K_s.

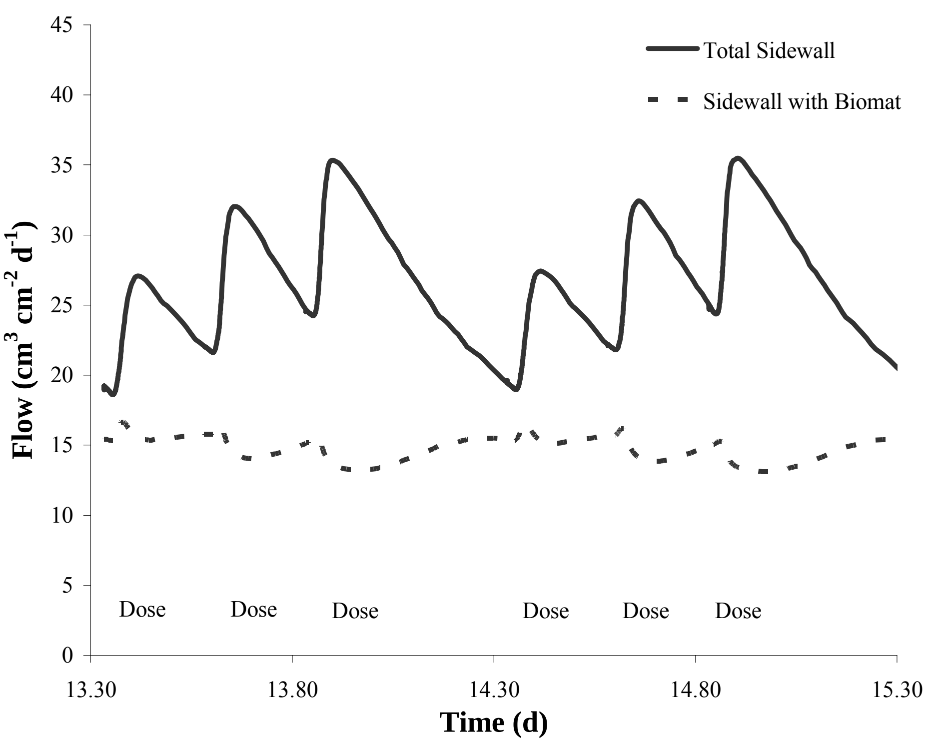

Figure 4-4. Total sidewall and sidewall with biomat flow of dispersal field in clay loam soil with equal trench bottom and sidewall K_s.

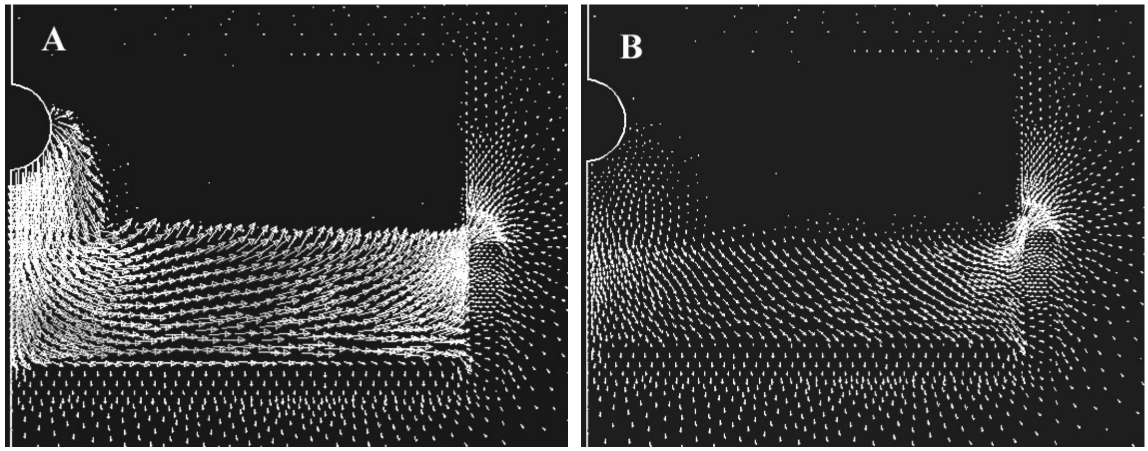

Figure 4-5. Velocity vectors for dispersal field in clay loam soil with equal K_s values for trench bottom and sidewall biomat. A-Dosing time is 2000 h with the highest ponding depth (11.2 cm). B-Resting period between doses with low flow.

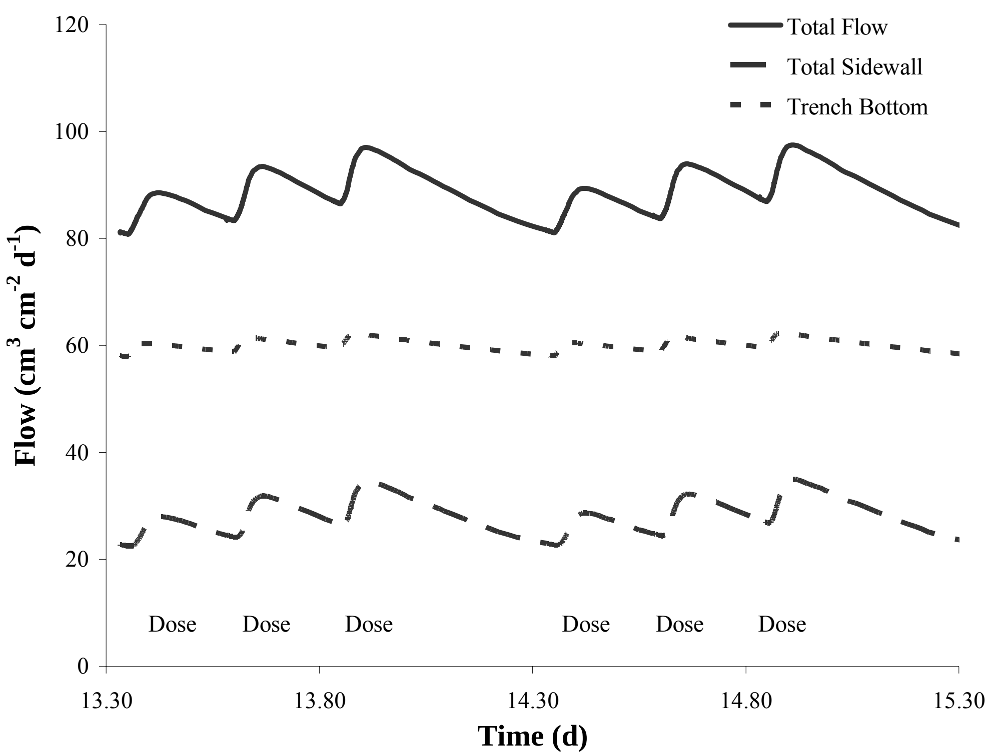

Figure 4-6. Total system flow, sidewall flow, and trench bottom flow of dispersal field in clay loam soil with 2 times the trench sidewall biomat K_s than the trench bottom biomat K_s.

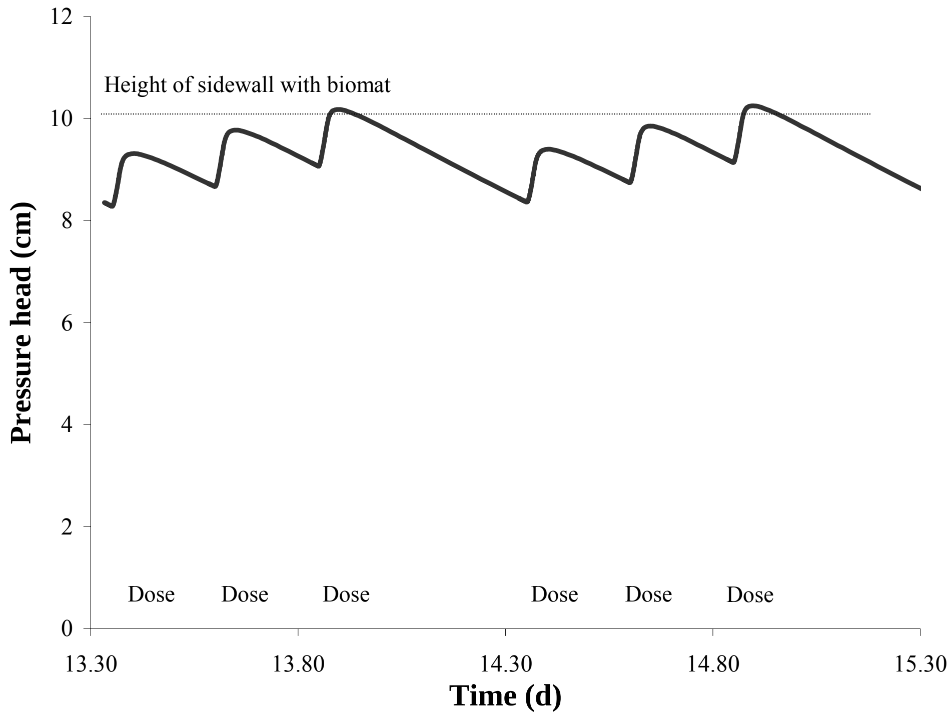

Figure 4-7. Pressure head (cm) of dispersal field in clay loam soil with 2 times the trench sidewall biomat K_s than the trench bottom biomat K_s.

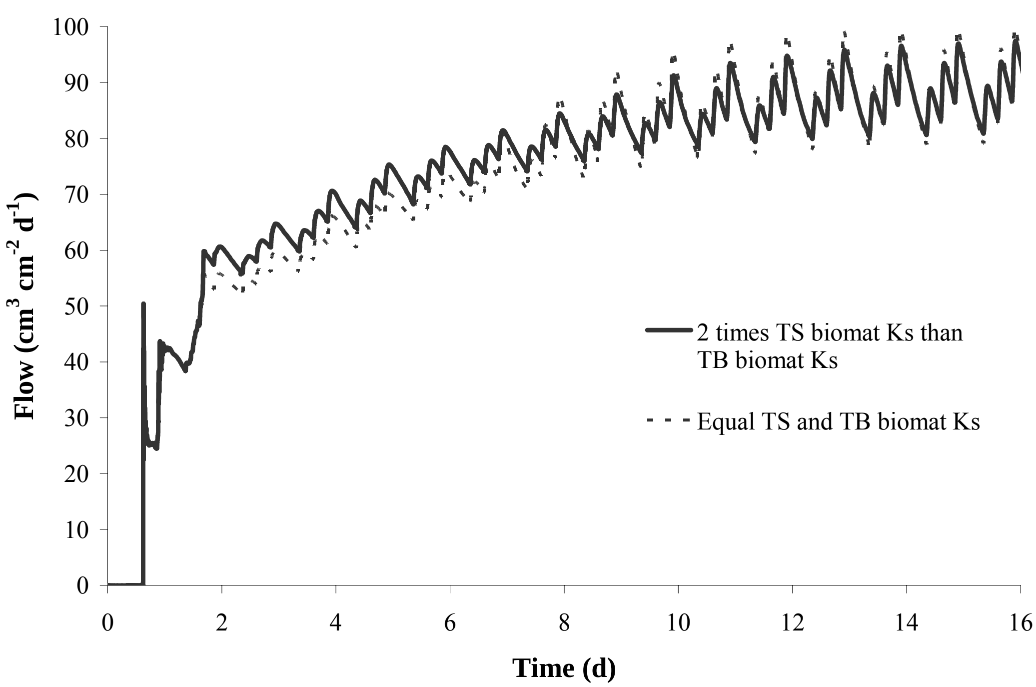

Figure 4-8. Total flow from time zero to steady state (13 d) for the clay loam flow simulations.

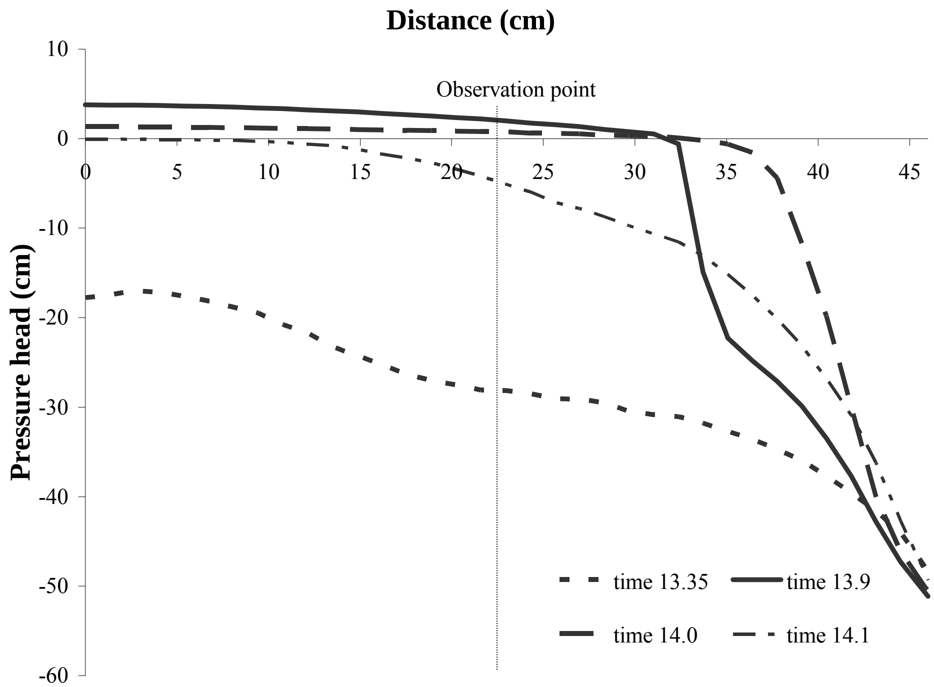

Figure 4-9. Pressure heads (cm) for different times (d) at the trench bottom of the dispersal field in sand soil.

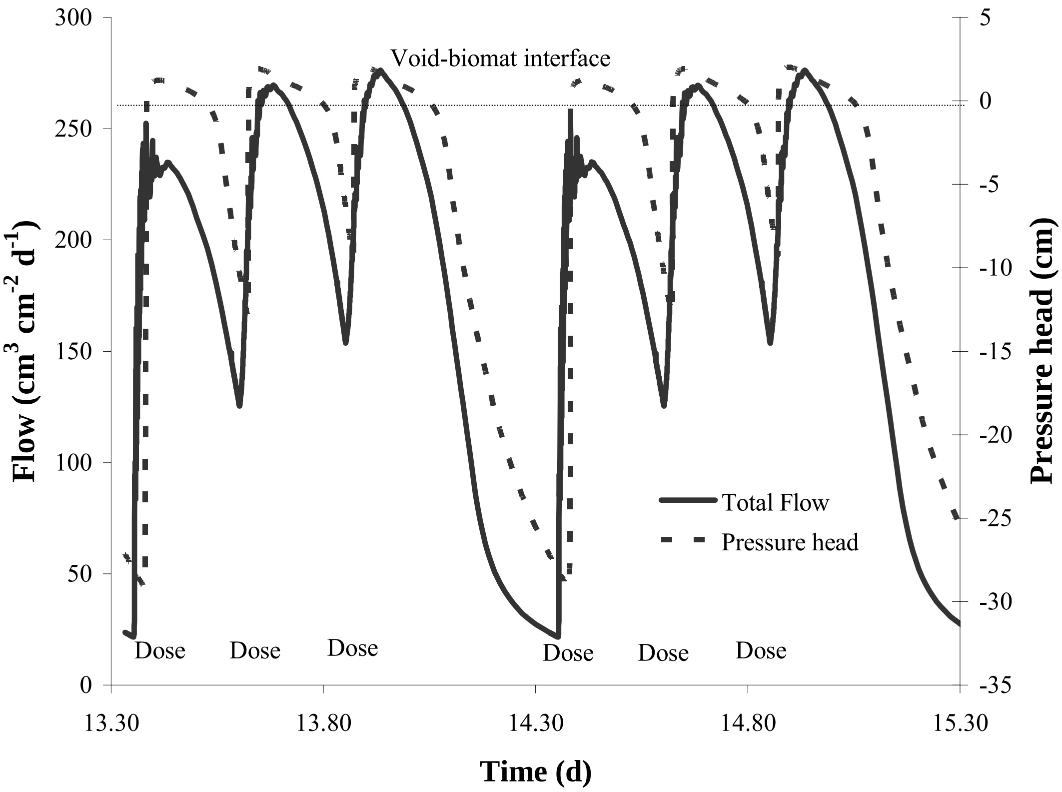

Figure 4-10. Total flow (cm/day) and pressure head (cm) of the dispersal field in sand-textured soil.

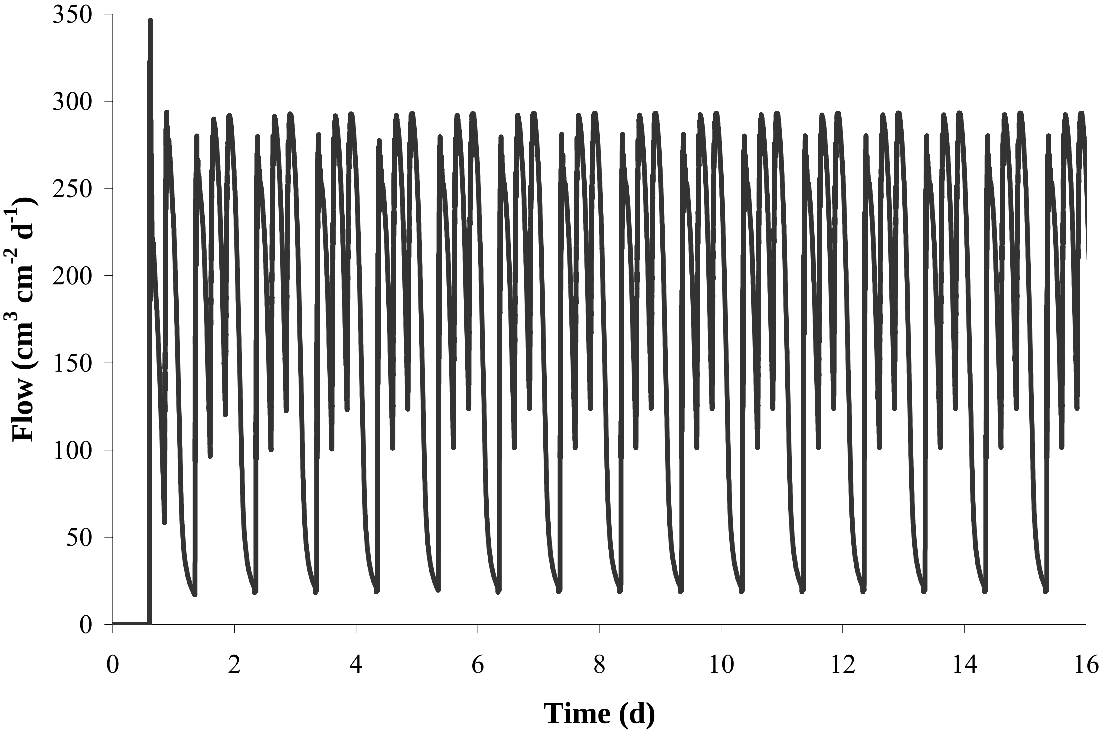

Figure 4-11. Total flow for time zero to steady state (2 d) representative of both sand models.

Table 4-1. Water retention and hydraulic conductivity parameters for the model simulations.

Model	Soil K_s	Bottom biomat K_s	Sidewall biomat K_s	Biomat resistance	n	α	θ_r	θ_s
	-------------cm d^{-1}	--------------		d				
measured‡	0.2	0.0§	0.0	81.5	1.09	0.07	0.09	0.45
clay loam 1	3.2	0.2	0.2	15.6	1.52	0.01	0.08	0.46
clay loam 2	3.2	0.2	0.4	7.5	1.52	0.01	0.08	0.46
sand 1	41	1.4	1.4	2.2	2.22	0.03	0.05	0.32
sand 2	41	1.4	2.8	1.1	2.22	0.03	0.05	0.32
aggregate	1000	NA†	NA	0.0	2.68	1.00	0.05	0.50

† Biomat was not incorporated into the gravel.
‡ Soil moisture release data measured from Sites D, E, and F from Chapter 3.
§ Measured biomat K_s and hydraulic resistance was representative of Site D only, due to the biomat-affected soil K_s being higher than the natural soil K_s at Sites E and F.

Table 4-2. Calculated flows from four model simulations.

Model	K_s trench sidewall versus bottom	Top	Sidewall with biomat	Total Sidewall	Trench Bottom	Input Flow	Output Flow
		---------------------------	----------cm^3 cm^{-2} d^{-1}	---------------------------			
clay loam 1	equal	0.5	14.5	26.5	62.0	90	88.5
clay loam 2	sidewall=2*TB	0.5	28.0	28.0	60.0	90	88.0
Sand 1	equal	0.0	0.0	0.0	179.6	180	179.7
Sand 2	sidewall=2*TB	0.0	0.0	0.0	179.6	180	179.8

References

Beach, D.N.H., and J.E. McCray. 2003. Numerical modeling of unsaturated flow in wastewater soil absorption systems. Ground Water Monit. Remediation 23:64-72.

Bouma, J. 1975. Unsaturated flow during soil treatment of septic tank effluent. J. Environ. Eng. Div. Am. Soc. Civ. Eng. 101: 967-983.

Keys, J.R., E.J. Tyler, and J.C. Converse. 1998. Predicting life for wastewater absorption systems. p. 167-176. *In* Proc. of the Eighth Natl. Symp. on Individual and Small Community Sewage Systems, 8th, Orlando, FL, USA. 8-10 Mar. 1998. ASAE Publ. 10-91:192-200. St. Joseph, MI.

Radcliffe, D.E., L.T. West, and J. Singer. 2005. Gravel effect on wastewater infiltration from septic system trenches. Soil Sci. Soc. Am. J. 69:1217-1224. Madison, WI.

Šimůnek, J., K. Huang, and M.Th. van Genuchten. 1998. The Hydrus code for simulating the one-dimensional movement of water, heat, and multiple solutes in variably-saturated media. Version 6.0 Res. Rep. 144. U.S. Salinity Lab., USDA-ARS, Riverside, CA.

USEPA. 2002. On-site wastewater treatment systems manual. EPA/625/R-00/008 Office of Water. Office of Research and Development. (Available on-line http://www.epa.gov/ORD/NRMRL/Pubs/625R00008/625R00008.pdf.) (Verified 13 Aug. 2002.)

White, K.D. and L.T. West. 2003. In-ground dispersal of wastewater effluent: The science of getting water into the ground. Small Flows Quarterly. 4 vol. no. 2

CHAPTER 5

CONCLUSIONS

Biomat formation in onsite wastewater management systems' (OWMS) dispersal field soil can reduce long-term wastewater infiltration rates. There is a lack of data on biomat K_s and thickness for common soils in Georgia; therefore, seven OWMS with mature dispersal fields, ranging in age from 7 to 43 yr, were sampled in the Georgia Piedmont (six sites) and Coastal Plain (one site) to evaluate the effect of biomat formation on natural soils. To complete this objective, saturated hydraulic conductivity (K_s) measurements were made on undisturbed cylindrical (7.6/9 cm diameter by 7.6/9 cm length) cores sampled from the trench bottom and sidewall of mature dispersal fields and from un-impacted soil adjacent to the trench. Polished blocks and thin-sections of undisturbed samples were used to evaluate biomat porosity and thickness. Biomat K_s was calculated by using the measured biomat thickness, soil thickness, natural soil K_s, and biomat-affected K_s. Model simulations were also used to measure two-dimensional flow through the trench bottom and sidewall of a dispersal field in Georgia Piedmont and Coastal Plain soil.

The K_s of the natural vertical and horizontally oriented soil samples were not statistically different (α=0.10). The natural soil K_s ranged from 0.0 (Site B) to 41 cm d^{-1} (Site G) with two of the sites (A and G) having acceptable wastewater acceptance rates (>2.8 cm d^{-1}). The biomat-affected soil taken from the trench sidewall and bottom were also not statistically different (α=0.10), even though sidewall samples were taken above the trench bottom where biomat thickness would be expected to be the greatest. The K_{eff} of the biomat-affected soil ranged from 0.2 (Site E) to 2.9 cm d^{-1} (Site G). Reduction in K_s occurred at four sites (Sites A, B, D, and G), with the reduction ranging from 34 to 93% of the natural soil K_s. The lack of reduction at the remaining sites was interpreted to be due to low K_s of the natural soil, natural variability in K_s, and variability in biomat development because of system design, system age, system installation, wastewater loading rates, and wastewater distribution.

Visual estimates of the biomat thickness ranged from <0.1 to >3 cm; however, biomat thicknesses ranged from 0.4 to 0.8 cm after quantitative measurements were made using fluorescence microscopy. The calculated biomat K_s ranged from 0.02 to 0.20 cm d^{-1} for Sites A, B, D, and G with hydraulic resistance ranging from 2.2 to 81.5 d. The biomat K_s was similar to the lower value (0.02 cm d^{-1}) reported by Keys et al. (1998). There was no statistical difference in van Genuchten's parameters at Site D and E, calculated from soil-moisture release curves, because the biomat volume was 4 to 9% of the total volume of the cores used for measurement.

For the clay loam simulation with equal trench sidewall and bottom K_s, as well as for the clay simulation with trench sidewall K_s being 2 times greater the trench bottom K_s, there was higher trench bottom flow (66.7 to 68.9%) than sidewall flow (29.4 to 31.1%). With twice the sidewall biomat K_s, ponding decreased and sidewall flow occurred only through the biomat-affected sidewall. There was 2.2% less trench bottom flow than the previous simulation that was attributed to more flow acceptance by the biomat-affected sidewall. Because the sidewall became unsaturated above the resting ponding depth, the sidewall had sharper increases in flow, after dosing, than the trench bottom. The trench sidewall flows in this study (0.32 to 0.62 cm d^{-1}) were similar to the trench sidewall flows (0.17 to 0.62 cm d^{-1}) of the clay textured soil reported by Bouma (1975). The trench bottom flows (0.17 to 0.75 cm d^{-1}) were much lower in Bouma's (1975) study.

Both sand-textured simulations had 99.8% of flow accepted by the trench bottom. Soil closest to the dispersal pipe accepted the wastewater flow, while the total sidewall and half the trench bottom remained unsaturated. Bouma (1975) reported higher flows for the trench bottom (5.8 to 7.5 cm d^{-1}) than the values reported in this study, which was attributed to the higher natural soil K_s.

Appendix A

Site A

Location: Forsyth County, GA at 34°10'36" N, 84°11'28"W

Type of System: Chamber Elevation: 351 m Date Sampled: 14 Aug. 2003

Geomorphic position: Upland Landform: Piedmont

Described by: Larry West

Fill--0 to 18 cm

Ap--18 to 31 cm; brown (10YR 4/3) sandy loam; weak medium granular structure; friable; very few fine roots; moderately acid (pH 5.6); clear smooth boundary

Bt--31 to 88 cm; red (2.5YR 4/6) clay loam; weak medium prismatic structure parting to weak medium subangular blocky structure; friable; few distinct clay films; few fine roots; very strongly acid (pH 5.0); gradual smooth boundary

BC1--88 to 127 cm; red (2.5YR 4/6) clay loam; weak medium subangular blocky structure; friable; few distinct clay films; few fine roots; strongly acid (pH 5.1); gradual smooth boundary

BC2--127 to 144 cm; yellowish red (5YR 4/6) clay loam; moderate medium red (2.5YR 4/6) depletions and strong medium light yellowish brown (10YR 6/4) depletions; weak medium platy structure parting to weak medium subangular blocky structure; friable; quartz dyke; moderately acid (pH 5.7); gradual smooth boundary

C--144 to 160 cm; dark yellowish brown (10YR 4/6) sandy loam; moderate medium yellowish red (5YR 4/6) concretions; moderate medium pale brown (10YR 6/3) depletions; moderate medium platy structure; friable; very strongly acid (pH 5.0)

Notes: Installed by hand, designed for 186 m^2 trailer, unused since March 2003, backhoe marks left lows in trench (samples obtained from lows), collembolans found feeding on biomat. No sidewall samples obtained.

Position 1: Trench bottom depth 133 cm. Biomat measured length 30 mm.

Position 2: Sampled toward the end of chamber. Flow lateral is clearer. Considerable root mat and growth. Ponding in this location.

Position 3: Trench bottom depth 147 cm. Top of chamber depth 111 cm and evidence of buckling. Platy structure beneath trench bottom.

Site B

Location: Forsyth County, GA at 34°10'36" N, 84°11'28" W

Type of System: EEE-ZZZ Lay 2003V Elevation: 365 m

Date Sampled: 23 Sept. 2003

Geomorphic position: Upland Landform: Piedmont Series: Appling/Cecil

Described by: Larry West

Ap--0 to 15 cm; dark grayish brown (10YR 4/2) sandy loam; weak medium granular structure; very strongly acid (pH 5.0); clear smooth boundary

Bt1--15 to 43 cm; red (2.5YR 4/6) clay; moderate medium subangular blocky structure; many medium roots; few distinct clay films on ped faces; strongly acid (pH 5.2); gradual smooth boundary

Bt2--43 to 102 cm; red (2.5YR 4/6) clay; few fine prominent yellow (10YR 7/6) mottles; moderate medium subangular blocky structure; few fine roots; strongly acid (pH 5.1); gradual smooth boundary

BC--102 to 173 cm; red (2.5YR 4/6) loam; many medium prominent yellow (10YR 7/6) mottles; weak medium subangular blocky structure; some relic foliations; strongly acid (pH 5.2); gradual smooth boundary

C--173 to 203 cm; red (2.5YR 4/6) sandy loam; many coarse prominent yellow (10YR 7/6) mottles; massive; very strongly acid (5.0)

Notes: Three bedrooms in trailer. Trailer removed 3 to 4 months prior to sampling. No garbage disposal. Depth to bottom of trench was about 175cm. Pipes crushed in 25 cm, which reduced the length of the trench.

Position 1: Trench bottom depth 175 cm. Good visible biomat. It rained the day before sampling. Water filled the pit after excavated.

Position 2: Trench bottom depth 150 cm. Sidewall samples have at least 3 cm of fill.

Site C

Location: Forsyth County, GA at 34°10’31”N, 84°11’27”W

Type of System: Gravel Elevation: 367 m Slope: 6% Shape: Concave/level

Date Sampled: 14 Oct. 2003

Geomorphic position: Upland Landform: Piedmont Series: Cataula without Btx

Hillslope component: side slope/shoulder

Described by: Tim Kring

A--0 to 5 cm; dark brown (10YR 3/3) sandy loam; moderate fine subangular blocky structure; friable; moderately acid (pH 5.7); clear wavy boundary

BA--5 to 20 cm; brown (7.5YR 4/4) sandy loam; moderate very fine subangular blocky structure; friable; about 3 percent rounded medium rock fragments; slightly acid (pH 6.1); gradual smooth boundary

Bt1--20 to 56 cm; red (2.5YR 4/6) sandy clay loam; moderate fine subangular blocky structure; firm; moderately acid (pH 5.9); gradual smooth boundary

Bt2--56 to 127 cm; red (2.5YR 4/6) clay; common distinct dark yellowish brown (10R 4/6) concentrations; common distinct yellowish brown (10YR 5/4) depletions; moderate fine subangular blocky parting to weak fine platy; firm; slightly acid (pH 6.3); gradual smooth boundary

Notes: The system was over 40 years old. Dimensions included 30 in wide trench and 10 in of gravel. This was a failed system.

Position 1: Trench bottom depth 91 cm. Wastewater effluent filled trench after excavation. Good visible biomat.

Position 2: Trench bottom depth 99 cm. Top of trench 66 cm. Good visible biomat.

Site D

Location: 115 Esterine Drive Warner Robins, GA 31093 in Houston County at 32°40’05”N, 83°42’15”W

Type of System: Gravel with four way distribution box Elevation: 135 m

Slope: 0% Date Sampled: 20 July 2004

Geomorphic position: Upland Landform: Coastal Plain Series: Faceville

Described by: Larry West, Vicki Hufstetler, and Shelby Finch

Ap--0 to 10 cm; Disturbed, mixed fill

E--10 to 24 cm; light yellowish brown (10YR 6/4) loamy sand; massive; very friable; slightly acid (pH 6.1); clear smooth boundary

BE--24 to 35 cm; yellowish red (5YR 4/6) sandy clay loam; weak moderate subangular blocky structure; friable; slightly acid (pH 6.1); gradual smooth boundary

Bt--35+ cm; red (2.5YR 4/6) sandy clay loam; weak moderate subangular blocky structure; friable; moderately acid (pH 5.8)

Notes: This system was distributing unevenly. No good visible biomat.

Position 1: Top of trench 65 cm. Bottom of trench 95 cm. Top of the water release cores at lower part of Bt horizon (78 cm).

Position 2: Top of trench 63cm. Bottom of trench 93 cm. Top of natural vertical soil 87 cm. Bottom of natural horizontal soil 82 cm.

Site E

Location: 4628 Braselton Hwy Hoschton, GA 30548-1705 at 34°04’24”N, 83°51’58”W in Jackson County

Type of System: Gravel Slope: 0% Elevation: 274 m

Date Sampled: 5 Aug. 2004

Geomorphic surface: Upland Landform: Piedmont

Described by: Larry West, Vicki Hufstetler, and Shelby Finch

Ap--0 to 15 cm; brown (7.5YR 4/2) sandy loam; weak fine granular structure; friable; many fine roots; strongly acid (pH 5.3); clear smooth boundary

Bt1--15 to 39 cm; red (2.5YR 4/6) clay; common medium yellowish red (5YR 4/6) depletions; common medium brownish yellow (10YR 6/8) depletions; moderate fine subangular blocky structure; friable; strongly acid (pH 5.3)

Bt2--39 to 84 cm; red (2.5YR 4/6) clay; common medium brownish yellow (10YR 6/8) depletions; few medium yellowish brown (10YR 5/4) depletions; moderate fine angular blocky structure parting to weak fine platy structure; friable; moderately acid (pH 5.8)

Bt3--84+ cm; yellowish red (5YR 4/6) sandy clay loam; common coarse red (2.5YR 4/6) concentrations; common medium brownish yellow (10YR 6/8) depletions; moderate medium platy structure parting to moderate medium subangular blocky structure; common thick clay films on horizontal ped faces; friable; strongly acid (pH 5.3)

Position 1: Trench Bottom depth was 76 cm. About 8 cm below the trench bottom, the soil was reduced to brown (10YR 5/3) and had few coarse pockets of red (2.5YR 4/6) interiors of natural peds. The soil was saturated at the time of sampling.

Position 2: Trench bottom depth was 65 cm. Weeping and worms present. The trench bottom’s soil color was brown (10YR 5/3), while the natural soil strong brown (7.5YR 4/6). Soil reduced to brown (10YR 4/3) beneath trench bottom (10-11) cm.

Position 3: Top of trench is 28 cm. Trench bottom is 48 cm. Gray soil below trench bottom is 3 cm. Linear streaks with 2 chroma depletions spaced at every 20 cm (vertical). Big prisms.

Site F

Location: 194 Snyder Road NE Milledgeville, GA 31061-9523 at 33°06’22”N, 83°07’01”W in Baldwin County

Type of System: Gravel Slope: 0% Date Sampled: 9 Aug. 2004

Geomorphic surface: Upland Landform: Piedmont Elevation: 117 m

Described by: Larry West and Vicki Hufstetler

Fill--0 to 9 cm

Ap--9 to 15 cm; dark yellowish brown (10YR 3/4) sandy loam; weak fine granular structure; friable; neutral (pH 6.9); clear smooth boundary

E--15 to 25 cm; yellowish red (5YR 4/6) sandy loam; weak fine subangular blocky structure; friable; neutral (pH 7.0); clear smooth boundary

Bt1--25 to 59 cm; red (2.5YR 4/8) clay; moderate medium subangular blocky structure; common thin clay films; friable; very strongly acid (pH 5.0); gradual smooth boundary

Bt2--59 to 96 cm; red (2.5YR 4/8) clay; common medium reddish yellow (7.5YR 6/6) depletions and few fine light brownish gray (10YR 6/2) depletions follow horizontal platy faces; weak moderate platy parting to weak moderate subangular blocky structure; friable; common medium clay films yellowish red (5YR 4/6) on horizontal and vertical faces; very strongly acid (pH 5.0); gradual smooth boundary

BC1--96 to 108 cm; red (2.5YR 4/8) clay loam; few medium light reddish brown (2.5YR 6/3) and few fine pale red (2.5Y 6/2) concentrations occur as horizontal streaks; weak moderate subangular blocky structure; friable; few faint clay films; strongly acid (pH 5.1); clear smooth boundary

BC2--108 to 130 cm; red (2.5YR 4/8) sandy clay loam; few medium light red (2.5Y 6/8) depletions and few fine light reddish gray (2.5Y 7/1) depletions; 2 cm thick of horizontal band of depletions; weak moderate subangular blocky structure; friable; few faint clay films; strongly acid (pH 5.2)

Position 1: Trench bottom depth was 135 cm. Top of trench was 104 cm. Water release cores were took at each horizon.

Position 2: Trench Bottom depth was 109 cm. Top of trench was 86 cm.

Site G

Location: 254 Hulett Wooten Farms Road Hazlehurst, GA 31539 in Jeff Davis County at 31°50’44”N, 82°33’59”W

Type of System: Chamber Slope: 0.5% Date Sampled: 9 Sept. 2005

Geomorphic position: Upland Landform: Coastal Plain Elevation: 73 m

Described by: Larry West and Shelby Finch

Fill--0 to 23 cm; dark grayish brown (10YR 4/2) loamy sand; very friable; many fine roots; moderately acid (pH 5.9); abrupt smooth boundary

A--23 to 36 cm; very dark gray (10YR 3/1) sand; pockets of yellowish brown (10YR 5/4); weak fine subangular blocky structure; very friable; slightly acid (pH 6.4); clear smooth boundary

Bh--36 to 53 cm; very dark grayish brown (10YR 3/2) loamy sand; weak fine subangular blocky structure; friable; moderately acid (pH 5.9)

Bh2--53 to 92 cm; dark gray (10YR 4/1) sand; weak moderate subangular blocky structure; friable; common light gray (10YR 7/2) depletions; neutral (pH 6.6)

B’--92 to 122 cm; grayish brown (10YR 5/2) loamy sand; weak moderate subangular blocky structure; friable; slightly alkaline (pH 7.4)

Bt--122 to 137 cm; gray (10YR 5/1) sandy loam; weak moderate subangular blocky structure; friable; slightly alkaline (pH 7.5)

Notes: Water table at 122 cm. Chamber system was full and had positive pressure. After opening the observation ports, a small amount of gas released and the wastewater rose above the top of the chamber system that ranged in depth from 36 to 38 cm from the soil surface. Trench bottom depths range from 56 to 64 cm and the soil beneath the biomat was yellowish brown (10YR 5/4) before drying.

Appendix B

Table 2. Particle Size Distribution of Site A (Forsyth County, GA)

Horizon	Depth	very coarse sand	coarse sand	medium sand	fine sand	very fine sand	total sand	total silt	total clay	pH
	cm	--------	--------	--------	--------	percent	--------	--------	--------	
Ap	18 to 31	3.4	5.3	13.1	24.4	12.6	58.8	29.4	11.8	5.6
Bt	31 to 88	1.5	3.0	8.7	15.4	9.4	38.0	27.6	34.4	5.0
BC1	88 to 127	2.1	4.3	9.2	14.7	13.9	44.2	27.5	28.3	5.1
BC2	127 to 144	0.6	2.8	6.4	10.5	11.4	31.8	39.9	28.3	5.7
C	144 to 160	2.6	6.8	11.3	19.2	18.7	58.6	27.9	13.5	5.0

Table 3. Particle Size Distribution of Site B (Forsyth County, GA)

Horizon	Depth	very coarse sand	coarse sand	medium sand	fine sand	very fine sand	total sand	total silt	total clay	pH
	cm	--------	--------	--------	--------	percent	--------	--------	--------	
A	0 to 15	1.8	5.6	14.8	21.2	9.5	52.8	28.9	28.3	5.0
Bt1	15 to 43	0.6	3.0	8.4	12.6	7.2	31.8	26.7	41.5	5.2
Bt2	43 to 102	2.7	2.9	7.5	11.9	8.6	33.7	23.4	42.9	5.1
BC	102 to 173	1.5	4.4	10.7	15.6	14.1	46.3	28.3	25.4	5.2
C	173 to 203	0.4	3.0	11.7	21.7	19.2	55.9	24.2	19.8	5.0

Table 4. Particle Size Distribution of Site C (Forsyth County, GA)

Horizon	Depth	very coarse sand	coarse sand	medium sand	fine sand	very fine sand	total sand	total silt	total clay	pH
	cm	--------	--------	--------	--------	percent	--------	--------	--------	
A	0 to 5	4.2	6.4	17.2	24.5	9.5	61.7	28.5	9.8	5.7
BA	5 to 20	2.2	6.2	16.8	26.9	11.0	63.0	23.0	14.0	6.1
Bt1	20 to 56	1.4	5.1	14.2	22.4	9.4	52.6	20.4	27.0	5.9
Bt2	56 to 127	1.6	3.7	8.9	13.5	6.3	34.0	18.0	48.0	6.3

Table 5. Particle Size Distribution of Site D (Houston County, GA)

Horizon	Depth	very coarse sand	coarse sand	medium sand	fine sand	very fine sand	total sand	total silt	total clay	pH
	cm	--------	--------	--------	--------	percent	--------	--------	--------	
E	10 to 24	3.1	10.4	15.6	35.7	15.5	80.3	14.3	5.4	6.1
BE	24 to 35	1.6	6.4	11.4	24.8	11.5	55.7	18.1	26.2	6.1
Bt	35+	1.6	5.7	9.3	20.6	9.9	47.1	14.7	38.2	5.8
Bt	78	2.6	6.7	9.5	21.2	10.2	50.2	12.3	37.5	5.5

Table 7. Particle Size Distribution of Site E (Jackson County, GA).

Horizon	Depth	very coarse sand	coarse sand	medium sand	fine sand	very fine sand	total sand	total silt	total clay	pH
	cm	---------------------------------percent---------------------------------								
Ap	0 to 15	3.3	10.3	21.2	23.7	8.4	66.9	19.1	13.9	5.3
Bt1	15 to 39	3.0	6.9	8.3	8.7	6.6	33.4	12.4	54.2	5.3
Bt2	39 to 84	2.6	7.1	8.9	8.3	5.4	32.4	13.4	54.3	5.8
Bt3	84+	2.0	7.1	8.6	7.7	5.7	31.1	13.6	55.2	5.3

Table 8. Particle Size Distribution for Site F (Baldwin County, GA)

Horizon	Depth	very coarse sand	coarse sand	medium sand	fine sand	very fine sand	total sand	total silt	total clay	pH
	cm	---------------------------------percent---------------------------------								
Ap	9 to 15	21.6	21.5	14.2	11.8	7.0	76.2	14.4	9.4	6.9
E	15 to 25	16.1	17.3	15.6	16.1	10.1	75.2	15.5	9.3	7.0
Bt1	25 to 59	11.4	8.3	5.9	6.2	5.3	37.2	19.0	43.8	5.0
Bt2	59 to 96	9.7	7.3	5.6	7.0	6.9	36.5	19.1	44.5	5.0
BC1	96 to 108	8.4	7.4	7.2	11.0	10.9	44.8	20.0	35.2	5.1
BC2	108 to 140	7.7	7.3	7.7	12.8	12.3	47.8	22.6	29.6	5.2

Table 9. Particle Size Distribution of Site G (Jeff Davis County, GA)

Horizon	Depth	very coarse sand	coarse sand	medium sand	fine sand	very fine sand	total sand	total silt	total clay	pH
	cm	---------------------------------percent---------------------------------								
Fill	0 to 23	1.0	8.9	29.1	31.8	13.3	84.1	3.8	12.1	5.9
A	23 to 36	0.9	9.2	27.4	34.6	14.2	86.3	2.1	11.5	6.4
Bh	36 to 53	1.9	9.4	26.0	32.5	13.2	82.9	2.5	14.6	5.9
Bh2	53 to 92	0.8	9.0	28.4	36.8	15.5	90.5	1.5	8.0	6.6
B’	92 to 122	1.1	10.0	26.8	31.7	13.3	82.8	1.7	15.4	7.4
Bt	122 to 137+	0.8	8.3	24.4	31.1	13.5	78.1	7.5	14.7	7.5

Appendix C

Table 10. Mean bulk density of Trench Bottom and Natural Soil

Site	Location	Trench Bottom Vertical Soil Bulk Density	Trench Bottom Horizontal Soil Bulk Density	Natural Soil Bulk Density
	county	--------------g cm^{-3}	---------------	
A	Forsyth	1.11	NA	1.28
B	Forsyth	1.24	1.22	1.28
C	Forsyth	1.49	1.22	1.36
D	Houston	1.55	1.55	1.52
E	Jackson	1.27	1.15	1.28
F	Baldwin	1.27	1.14	1.35
G	Jeff Davis	1.64	NA	1.75